THE PENNSYLVANIA STATE UNIVERSITY
SCHREYER HONORS COLLEGE

DEPARTMENT OF MECHANICAL AND NUCLEAR ENGINEERING

REDESIGN TO REDUCE MASS: WALLOPS ARC-SECOND POINTER (WASP)

CAITLIN E. GIBBONS
SPRING 2016

A thesis
submitted in partial fulfillment
of the requirements
for a baccalaureate degree
in Mechanical Engineering
with honors in Mechanical Engineering

Reviewed and approved* by the following:

Sean Brennan
Associate Professor of Mechanical Engineering
Thesis Supervisor

Zoubeida Ounaies
Professor of Mechanical Engineering
Honors Adviser

* Signatures are on file in the Schreyer Honors College.

ABSTRACT

Scientists have used balloons to study earth for a long time now; however, the Wallops Arc-Second Pointer (WASP) is a significant advancement to present pointing apparatuses for planetary scientists in particular because they require a highly stable pointing system to accurately track planetary targets as they move in the solar system. Additional examples of objectives include exoplanets and X-ray sources outside the solar system. WASP is an innovative and standardized system that can accurately point a balloon payload within a sub arc-second; 70^{o} in the pitch direction and 15^{o} in the yaw direction. WASP has successfully completed three test flights, in 2011, 2012 and 2013. WASP is already a completely functional and operating system, however the Balloon Program Office (Code 820) and the Mechanical Systems Branch (Code 548) at the National Aeronautics Space Administration (NASA) Wallops Flight Facility (WFF) would like to improve upon the original structure. The current version of WASP weighs approximately 600 lbm. NASA WFF intends to reduce the weight the pointing system by at least a 100 lbm, while maintaining the original strength and stiffness. Reductions in weight will allow project scientists to incorporate additional instruments to a payload, or by flight operations for a longer duration flight. The end goal of redesigning WASP is to create a system that will be included in a standardized balloon platform for earth science, planetary science, and for proposals such as the Gondola for High Altitude Planetary Science (GHAPS) project.

The thesis details the research conducted, redesign decisions for WASP, a suggested assembly procedure for the inner frame of the WASP, finite element analysis (FEA) conducted on the inner frame, and recommendations for moving forward. The redesigned version of WASP is 161 lbm, or 31% lighter than the original design. The redesigned WASP inner frame utilized

standard off-the-shelf extrusions to maintain cost-effectiveness. FEA was conducted using Autodesk Inventor Pro and Abaqus. The stress analysis tested the redesigned version under an applied load of 1,500 lbf loading with a factor of safety of 10 (15,000 lbf load), to ensure that the structure would not experience ultimate failure. The analysis using Inventor demonstrated that there was a 13.5% difference between simplified hand calculations and the FEA. The percent difference between the Abaqus FEA and the hand calculation was approximately 2.4%. The redesigned WASP met all the project requirements, and was approved for manufacture by the NASA WFF Mechanical Systems Branch engineers and technician.

TABLE OF CONTENTS

LIST OF FIGURES

LIST OF TABLES

ACKNOWLEDGEMENTS

Mom and Dad, without your continual encouragement and care I would not be the person I am today. Thank you for the countless late nights you stayed up to help me understand my homework or help me put finishing touches on a project before it was due. Thank you for imparting and fostering a love of learning throughout my entire life. And most importantly, thank you for always believing in me, even when I did not believe in myself. You both are the best teachers and role models I have ever had, "I love you right up to the moon — and back." ~ Sam McBratney

Special thank you to Code 548 for providing me with the thesis topic, and for all of the support and guidance you gave me throughout the design and analysis process. Particularly thank you to the following individuals:

Chris Shreves, Mentor and Branch Technologist | NASA Wallops Code 548

Leyland Young, Aerospace Engineer | NASA Wallops Code 548

Chris Strickland, Associate Branch Head | NASA Wallops Code 548

Dr. Jerry Sterling, Branch Head | NASA Wallops Code 548

Thank you to the following individuals for their assistance in completing the analysis:

Dr. Reuben Kraft, Assistant Professor | Penn State MNE Department

Clayton Hofmockel, Bryan Griffin, Yuanhui (Riley) Zhang | M E 461 Team

Chapter 1

Introduction

Objective

The NASA Wallops Flight Facility (WFF) Mechanical Systems Branch's main goal for redesigning the Wallops Arc-Second Pointer (WASP) structure was to reduce the weight by at least 100 lbm, about 18% lighter than the original, while maintaining the stiffness and strength of the original design. Reducing the weight of the pointing system would afford two significant options for a balloon mission. Project scientists could choose to either include more instruments on the payload or opt for a longer duration flight; both would increase the amount of data collected during a mission. An initial brainstorming session identified ideas to decrease the weight; the ideas included: a change in shape/geometry, change in material, and center mounting the hub motors to eliminate the need for counterweights on the inner frame. The redesign had to continue being cost-effective, by including hardware that could be purchased off-the-shelf. The original structure acted as a benchmark for every redesign decision.

Background Information

WASP is an innovative and standardized system that can accurately point various different balloon instruments. It is a highly stable and flexible system with sub arc-second accuracy (less than 1/3600 of a degree). WASP integrates with a balloon platform that flies in the

stratosphere—at altitudes between 110,000 to 130,000 ft, which is above approximately 99.5% of Earth's atmosphere. [1] The major customers interested in incorporating WASP into missions include earth science, planetary science, and the Gondola for High Altitude Planetary Science (GHAPS) project. The WASP assembly has been revised three times in its history, after test flights of the system (in 2011 and 2012) and a successful flight with a science instrument (2013). The current version, and what will henceforth be referred to as the original structure, was used for balloon payloads from 2014 to present day (see Figure 1). [2]

Two types of the original structure were offered to the customer: an unstretched version, at 53.25", and its stretched version, at 62.5". The unstretched version is lighter; however, a stretched version could be utilized to accommodate larger payloads. Once the WASP inner frame was redesigned, the structure was reduced in weight by 161 lbm. An additional model was redesigned to provide a stretched version of the inner frame, and compared to the original structure, the redesign reduced weight by 156 lbm. The stretched version of the inner frame would provide greater flexibility in size for potential science payloads. To reduce the scope of this thesis, FEA was performed only

Figure 1: Original WASP Integrated on a Balloon Platform

on the un-stretched version of the redesigned frame to ensure that it did not experience ultimate failure (reaching maximum ultimate tensile strength).

Customer Needs and Specifications

WASP was intended to be a standardized pointing system for any balloon-borne platform for easy manufacture and utilization by a variety of customers. The main redesign considerations for WASP included weight, maintained stiffness, maintained strength, cost-effectiveness, machinability, and ease of assembly. There were no values provided to correspond with each specification; however, the structure could not experience ultimate tensile or yielding failure. The original WASP served as a benchmark for weight reduction and sustained stiffness and strength. The internal frame beam geometry was selected because it was a standard off-the-shelf part, which is more cost-effective than a customized part. The redesigned versions of WASP presented in the thesis were submitted to the NASA Mechanical Systems Branch machinist, who approved each part's machinability and the ease of assembly for the structure as a whole.

Chapter 2

Concept Development

Geometry Selection

The original WASP frame (see Figure 2) utilized a hollow rectangular frame; therefore, the hollow rectangular tube was compared to other hollow geometries to determine which cross-section met the weight and stiffness requirements. Hollow structures are generally stronger than their solid counterparts, on an equivalent-weight basis. The two factors considered in Figure 3

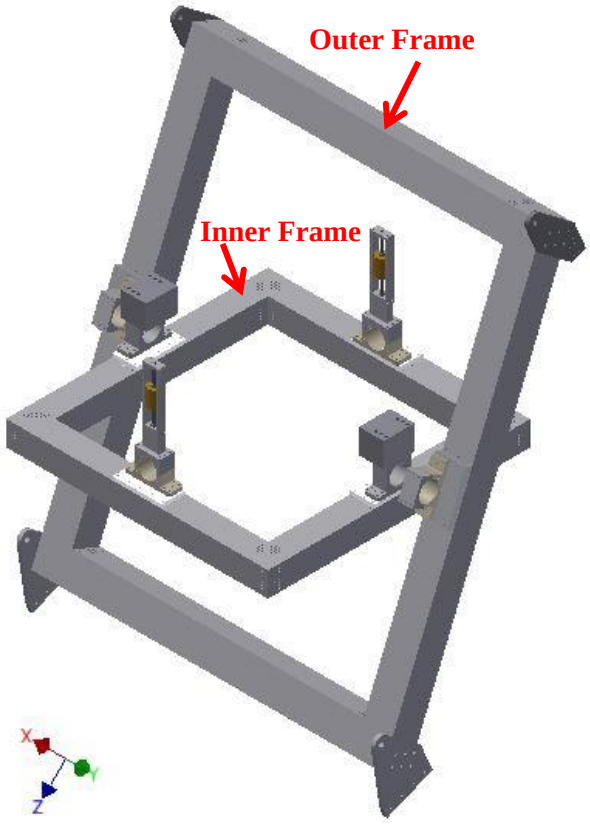

Figure 2: Original WASP Structure

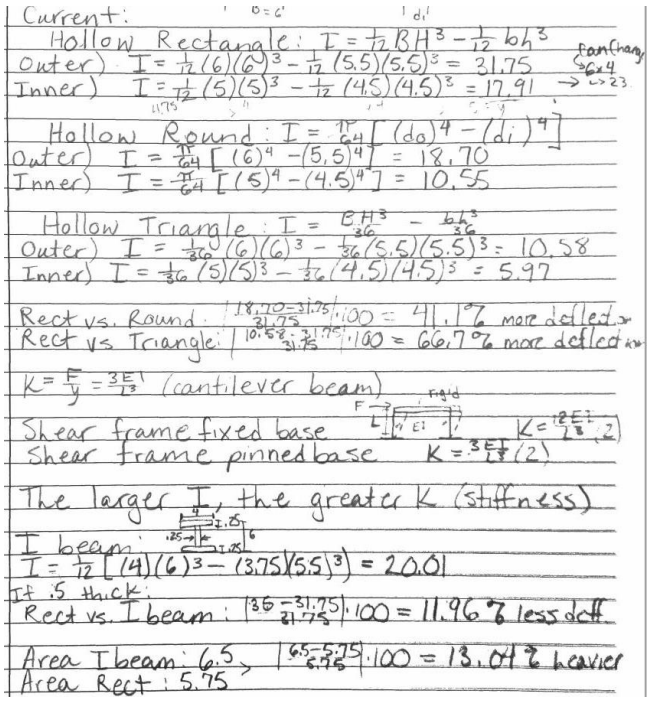

Figure 3: Hand Calculations Preformed to Compare Geometric Structures

are area moment of inertia (I) and cross sectional area. The area moment of inertia is an important factor when determining the stiffness of a beam or frame; the greater the I, the stiffer the structure. To evaluate the weight lost or increased, the cross sectional areas were compared (smallest area will be lighter). The hollow rectangle had largest area moment of inertia (I), and therefore the stiffest structure. To maintain the same amount of stiffness, the structure should be made from a rectangular tube.

The original structure's inner frame dimensions were 5x5x0.25". The force will be applied normal to the top surface of inner frame beams at a maximum loading condition. If the height—or the dimension that spans across the central horizontal axis—was increased (see Figure 4), the beam would have greater strength to oppose a downward force. Not as much material would be necessary if the stiffness was increased; thus, the structure could be thinner, which decreases the overall weight.

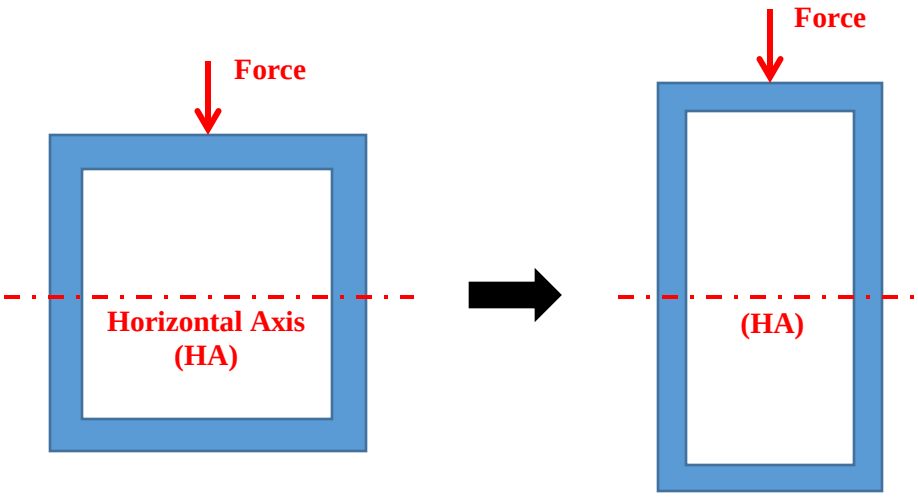

Figure 4: Depiction of Increasing Height across the Horizontal Axis

Three iterations to reduce the weight of the WASP inner frame were created to test which had the most weight savings, with minimal impact to stiffness. The first iteration reduced the

weight of the overall structure by 25% and the second iteration by about 29%. While both of these iterations had positive stiffness percent difference calculations, they were created using tubing that was not standard off-the-shelf. Consequently, they were not cost-effective. The third iteration only considered standard off-the-shelf tubing, as displayed in Table 1.

Table 1 presents a comparison of the various standard off-the-shelf extrusion dimension choices. The top row, in light blue, is the original structure's dimensions; this is the baseline for all of the calculations. The table is color coded to demonstrate desirable values in increasingly darker shades of green and less desirable values in increasingly darker shades of red. The equations used to create Table 1 are numbered (1) – (4) in Appendix C.

Table 1: Percent Difference Calculations for Weight and Stiffness of Standard Extrusion Dimensions

H	B	h	b	A	I	% Weight	% Stiffness
5.00	5.00	4.50	4.50	4.75	17.91		
6.00	4.00	5.50	3.50	4.75	23.47	0.00	31.06
6.00	4.00	5.75	3.75	2.44	12.59	-48.68	-29.71
6.00	3.00	5.63	2.63	3.23	15.07	-31.91	-15.88
6.00	2.00	5.50	1.50	3.75	15.20	-21.05	-15.12
6.00	2.00	5.75	1.75	1.94	8.28	-59.21	-53.80
8.00	4.00	7.50	3.50	5.75	47.62	21.05	165.86
8.00	3.00	7.50	2.50	5.25	40.11	10.53	123.93
8.00	**2.00**	**7.75**	**1.75**	**2.44**	**17.45**	**-48.68**	**-2.58**
5.00	3.00	4.50	2.50	3.75	12.27	-21.05	-31.52

None of the options displayed in Table 1 provided an ideal outcome of both weight reduction and maintained stiffness. However, the 8x2x0.125" geometry (bolded row) had the most predicted weight reduction with the least amount of deflection thus was selected for the third iteration of the WASP inner frame.

Material Selection

Research was conducted on carbon fiber, honeycomb core, steel alloys, and aluminum alloys to explore which material would be best for the frame. Material requirements included cost-efficiency, standard off-the-shelf parts, lightweight, durability, and functionality at low temperatures.

Carbon fiber is an extremely lightweight and stiff material. The larger the modulus of elasticity the greater the stiffness; the Young's modulus of carbon nanotube, single-walled can vary, but is generally around 145 ksi. [3] However, it is an extremely expensive material to buy off-the-shelf or manufacture. Carbon fiber would be too cost-prohibitive to use for the framework of WASP. Additionally, any weight loss would be negligible because each tube would require significant aluminum or titanium mounts/connectors to join together, and to secure the hub motors to the resulting frame. The mixture of two or more materials would introduce the risk of individual parts expanding and contracting at different rates due to any thermal fluctuations the telescope may experience during flight.

Honeycomb core is lightweight and performs exceptionally well under compressive stress. Unfortunately, it performs poorly when a sheer stress acts upon it. [4] Specifically—using material properties, dimensions, and equations outlined in *HexWeb™ Honeycomb Sandwich Design Technology*—the maximum shear stress of one beam would equal approximately 466 psi. [5] Furthermore, the calculations proved that the total maximum deflection experienced would cause a honeycomb beam to fail. Figure 5 displays the equations for a center loaded honeycomb beam provided from the HexWeb document. Table 3 in Appendix A details the results from these calculations.

Bending Stiffness

$$D = \frac{E_f t_f h^2 b}{2}$$

Where $h = t_f + t_c$

Shear Stiffness

$$S = b h G_c$$

As the core shear here will be taken by the weaker transverse direction - take $G_c = G_w$ shear modulus

Facing Stress

$$\sigma_f = \frac{M}{h t_f b}$$

Where M is Maximum Bending Moment expression from page 11

and $h = t_f + t_c$

Deflection

$$\delta = \underbrace{\frac{k_b P l^3}{D}}_{\text{Bending}} + \underbrace{\frac{k_s P l}{S}}_{\text{Shear}}$$

Where k_b and k_s are deflection coefficients from page 11.

If doing preliminary calculations, just work out the bending deflection.

If optimising design, calculate for both bending and shear components (as shown opposite).

Core Stress

$$\tau_c = \frac{F}{hb}$$

Where F is Maximum Shear Force expression from page 11

Figure 5: Equations Used from *HexWeb™ Honeycomb Sandwich Design Technology*

Stainless steel alloys have much greater modulus of elasticity and Ultimate Tensile Strength (UTS); therefore the structure may not need as much material to maintain stiffness and strength. However, the main concern with steel—especially ferritic and martensitic stainless steels—is that it becomes very brittle at low temperatures. [6] Decreasing temperature can adversely affect the tensile toughness of many commonly used steel alloys. Most high tensile steel alloys, such as QT-100 Steel, are not recommended for structural use below -45°C; which does not meet the general balloon program standard of -90°C. [7] Consequently, steel could fail depending on the flight environment selected.

The current frame design utilizes a hollow rectangular tube made from 6061-T6 aluminum. 6061-T6 aluminum is one of the most commonly used aluminum alloys due to its strength, heat treatability, comparatively easy machining, weldability, and capability for

annealing. In addition, aluminum alloys do not become brittle at low temperatures; as the temperature decreases tensile and yield strength increase. [8] If all of the brackets and framework were manufactured from 6061-T6 aluminum, it would reduce the risk of individual parts expanding and contracting at different rates due to any thermal variations in the stratosphere. Hence, the redesigned structure will continue to use 6061-T6 aluminum.

Theoretical Analysis

Verification was required to ensure that the redesigned WASP inner frame—with new dimensions of 8x2x0.125" (refer to Chapter 1: Geometry Selection)—would not experience ultimate failure throughout flight. WASP could experience a maximum load of 1,500 lbm during a mission; however, the Balloon Program Office mandated that WASP must meet a factor of safety equal to 10. The 10 G load requirement was based on parachute opening-shock at mission termination. Hence, the WASP frame should not experience ultimate failure at a 10 G load.

The original structure—unstretched at 53.25" and its stretched version at 62.5"—never came close to experiencing ultimate failure. Therefore, they were both used as the baseline for 1 G and 10 G cases (see Tables 4 and 5, Appendix A). The frame is a linear model, thus it follows the principle of superposition. Hence the frame could be separated, and only one individual beam needed to be examined. To obtain a rough estimate of whether the structure would fail at UTS, the maximum stress hand calculations were simplified to modeling one simply supported beam. To ensure that the structure would not fail, the percent difference between the maximum stress and the material UTS could not lie within the normal engineering standard significance of two sigma, or $\pm$5%. The new version of the frame, both un-stretched and stretched, were well

above two sigma and therefore would not experience ultimate tensile or yielding failure (see Tables 6 and 7, Appendix A). Equations (5) – (9) in Appendix C were used to find the maximum bending stress, percent difference, and margin values listed in Tables 4 – 7.

Summary of Design Decisions

The hub motors were mounted on top of the inner frame for the original structure (see Figure 6). Counterweights were required to compensate for the motors not being in line with the frame's center of gravity. The redesigned inner frame structure center mounted the hub motors, which placed them in line with the frame's center of gravity (see Figure 7). By center-mounting the motors, the counterweights became unnecessary. The method to attach the motors—a saddle-mount assembly—to the frame remained relatively similar because it allowed greater flexibility in alignment for the technician who would assemble the structure. L-shaped mounting brackets and a

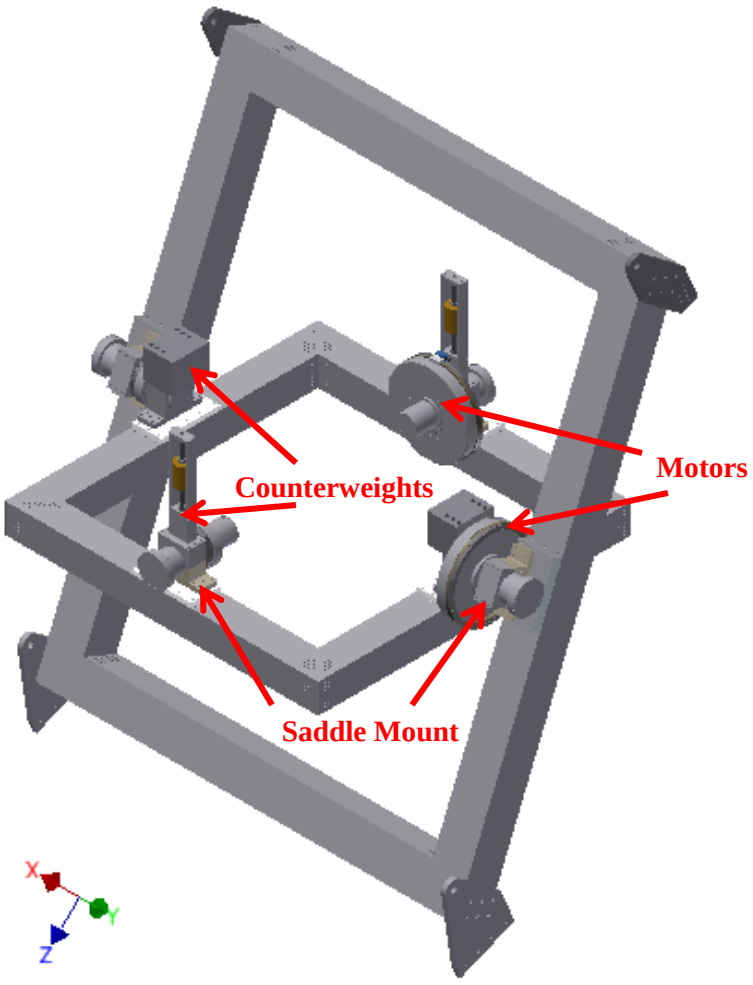

Figure 6: Original WASP Structure with Motors

faceplate secured the saddles to the inner frame. Tolerance was built into each mounting assembly, which allowed the technicians to easily adjust the alignment of the telescope. Reinforcement plates were designed for each joint and cutout in a beam.

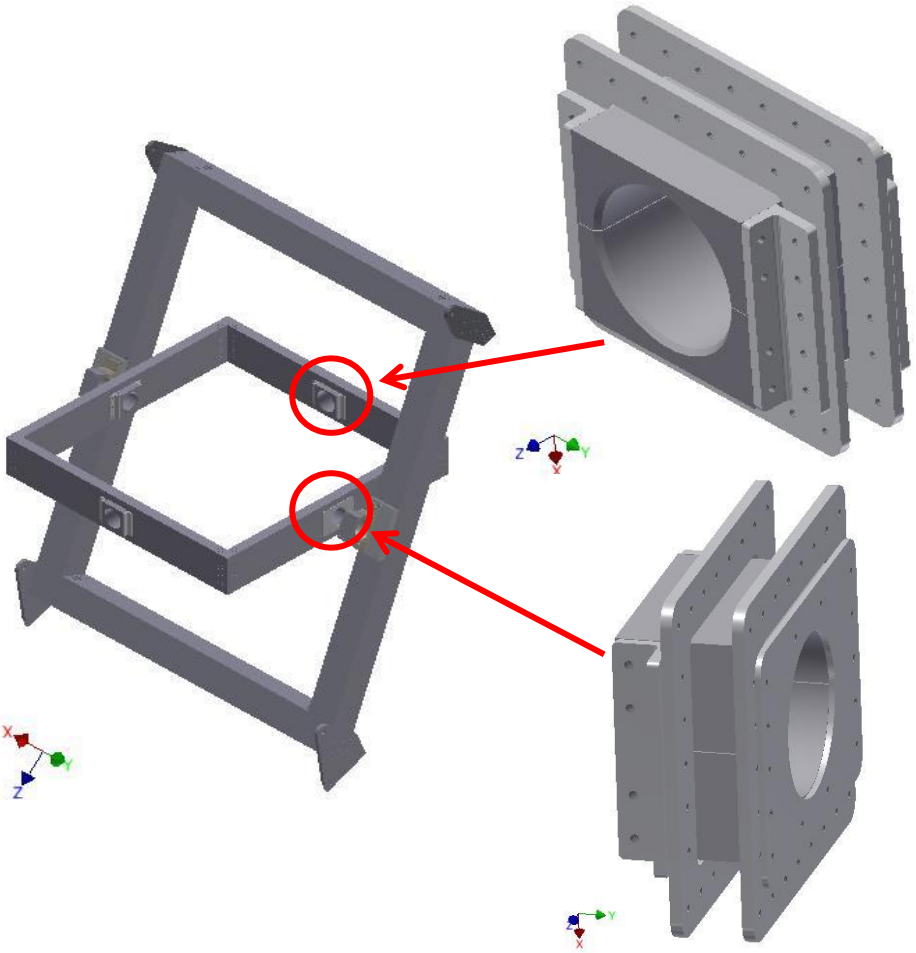

Figure 7: Positions of Yaw (Top Right) and Pitch (Bottom Right) Saddle Mounts for Hub Motors

The redesigned WASP inner frame also differed from the original structure due to new dimensions chosen specifically to reduce weight (see Figures 8 and 9). The redesign process underwent three iterations. The first two iterations focused on weight savings and did not comply with standardized off-the-shelf extrusions. To reduce cost, the final dimensions were based on

standard off-the-shelf rectangular 6061-T6 aluminum tubes. The structure will continue to be built from 6061-T6 aluminum because it is cost-efficient, lightweight, durable, and functional at low temperatures. A stretched version of the inner frame was designed to provide greater flexibility for prospective payloads; such as having a larger primary mirror.

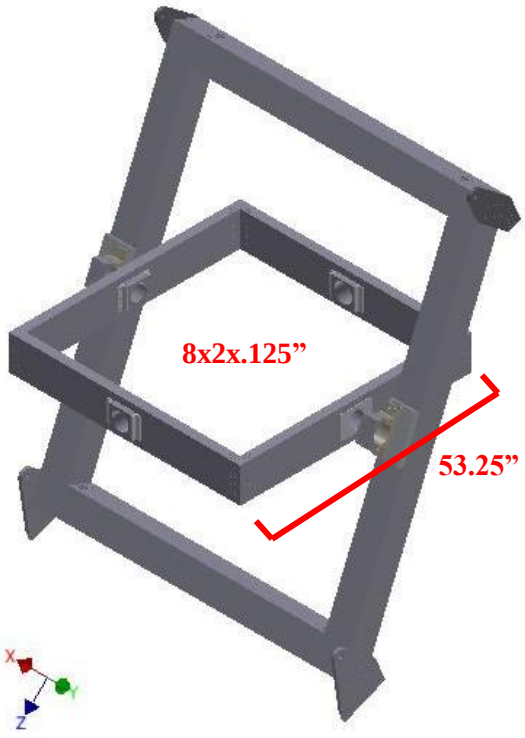

Figure 8: Un-stretched Redesign of WASP

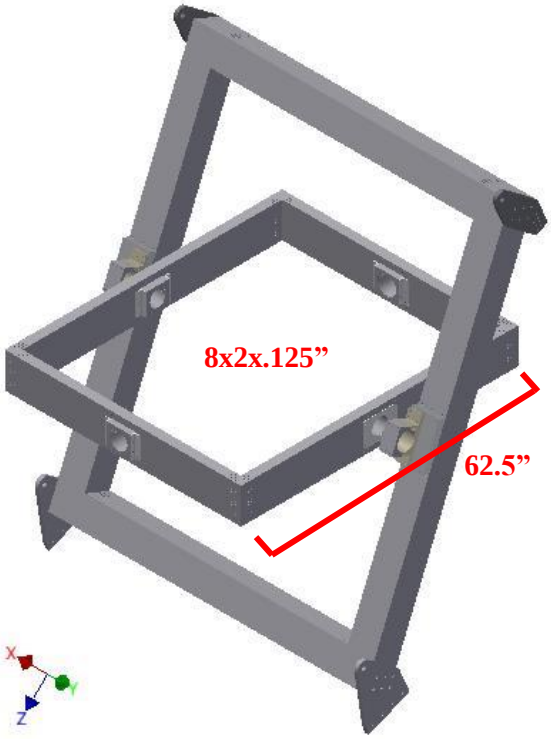

Figure 9: Stretched Redesign of WASP

The design changes accomplished the main objective of reducing the weight by at least 100 lbm. The un-stretched version was approximately 161 lbm, 31% lighter than the original, and the stretched version was about 156 lbm, or 30% lighter than the original. Reducing weight of WASP is important because it provides project scientists or flight operations with the option to either include more instruments on the payload or hold a longer duration mission.

Chapter 3

Detailed Design Assembly

Detailed Drawings

The entire assembly, un-stretched, is depicted in Figure 10. Detailed drawings were made for manufacturing (see Figures 43 – 56, Appendix B).

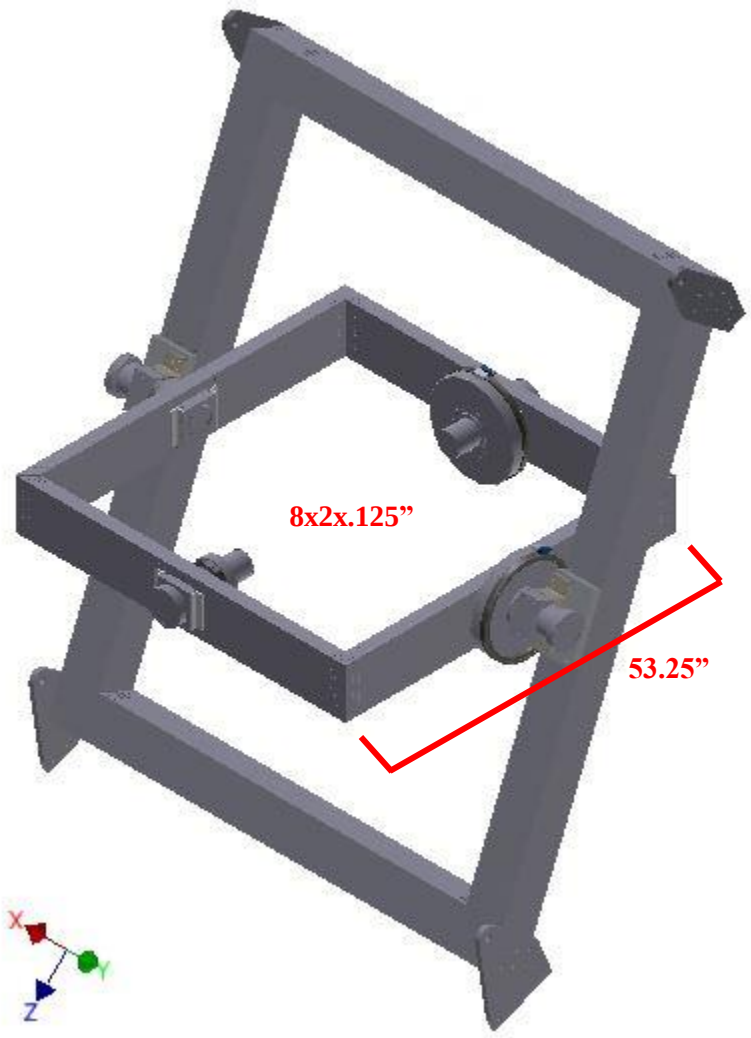

Figure 10: Complete Un-Stretched WASP Assembly

Assembly Procedure

The assembly procedure describes steps for assembly of the WASP inner frame.

1. Slide the inner mounting plates inside each of the beams. There should be one plate around each center cut.
2. Do not rivet the five vertical rivet holes on either side of the inner mounting plates until the motors, saddles, and outer mounting plates/brackets are in place.
3. Rivet plates in place using the top and bottom horizontal rows of holes (see Figure 11)

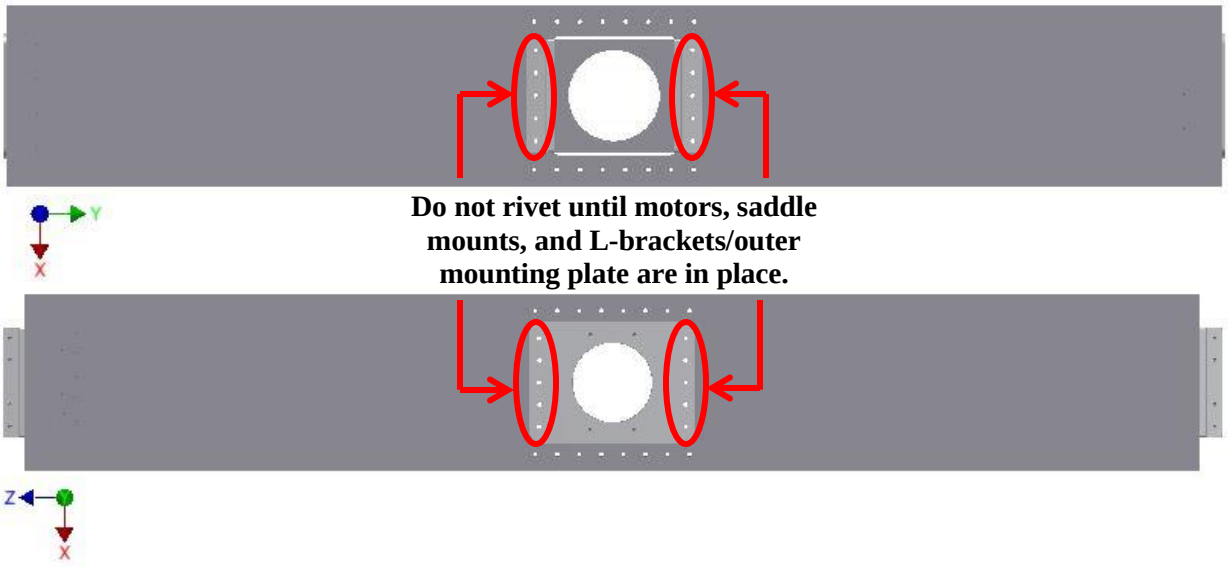

Figure 11: Yaw Beam (Top) and Pitch Beam (Bottom)

4. Position two "Doubler Side Standard" reinforcement plates at the end of every beam. One is for the top surface, the other is for the bottom surface (see Figure 12). Rivet in place.

5. Position a “Doubler Corner Outer” plate at the end of every beam towards the outside of the beam (see Figure 12). Rivet in place.
6. Position a “Doubler Corner Inner” plate at the end of every beam towards the inside of the beam (see Figure 12). Rivet in place.
7. Place two beams together, so that each joint has one set of reinforcement plates, and rivet the assembly together (see Figure 13).

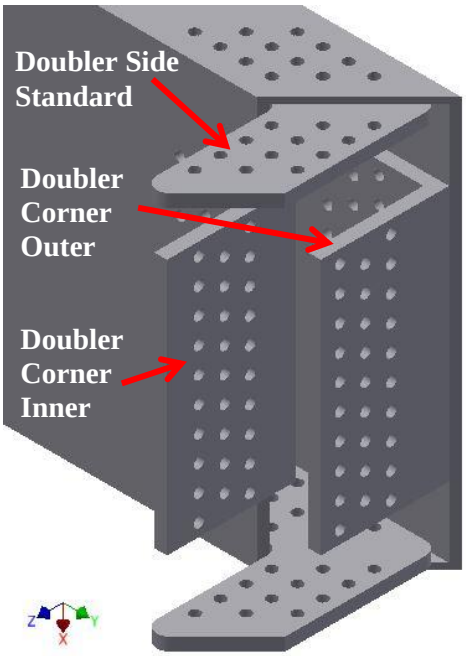

Figure 12: Joint Reinforcement Plates

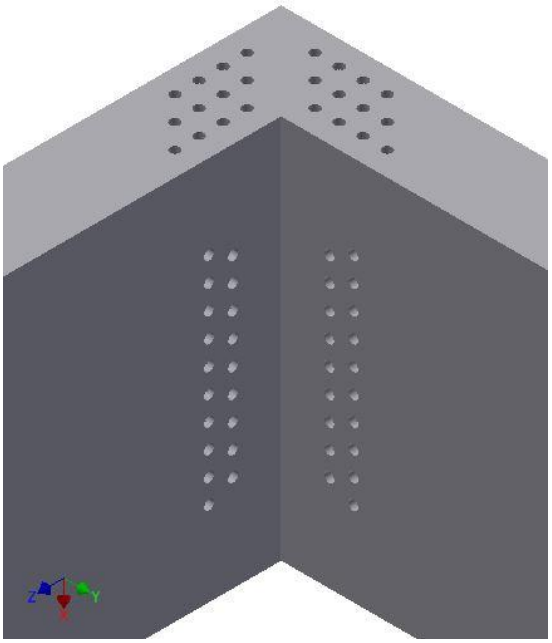

Figure 13: Beams Riveted Together

Beams on Yaw Axis:

8. Place the yaw top and bottom hub saddle bracket (larger than the pitch saddle bracket) around the top shaft of the hub motors. Use 10-32 screws to fasten the top saddle to the bottom, make sure that the screws lie flush.

9. Slide the saddle through the rectangular slot in the beam, from the inside of the frame (so that the rotary motor is inside the frame).
10. Use 10-32 screws to fasten the yaw hub L-brackets to the saddle mounts on both sides of the frame (see Figure 14).

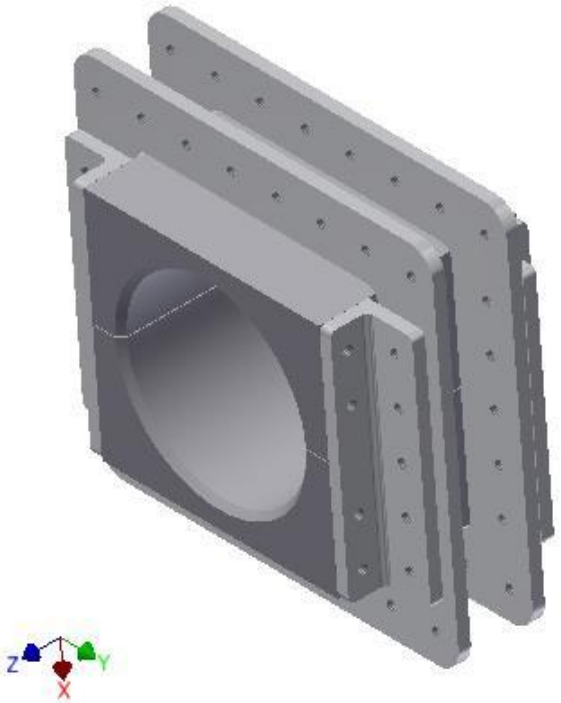

Figure 14: Yaw Saddle Mount for Hub Motors

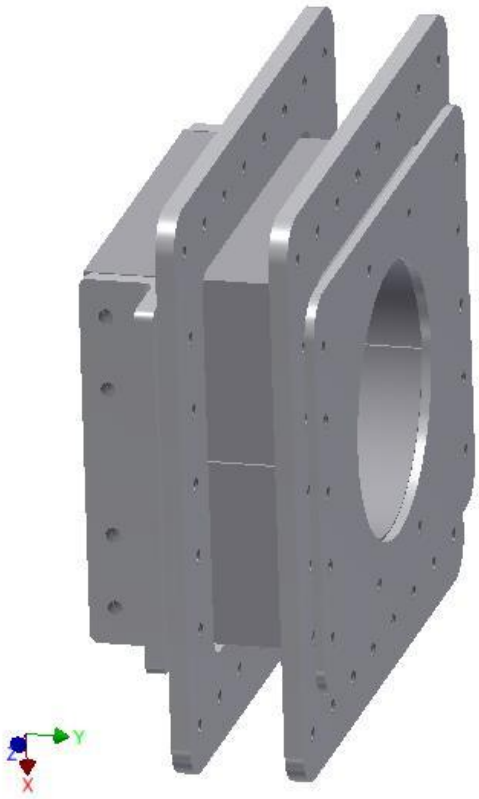

Figure 15: Pitch Saddle Mount for Hub Motors

11. Use rivets to secure the L-brackets to the frame and inner mounting plate (see Figure 11).

Beams on Pitch Axis:

12. Place the pitch top and bottom hub saddle bracket around the bottom shaft of the hub motors. Use 10-32 screws to fasten the top saddle into the bottom, make sure that the screws lie flush.

13. Slide the saddle through the rectangular slot in the beam, from the outside of the frame (so that the rotary motor is outside the frame).
14. Use 10-32 screws to fasten the pitch hub L-brackets to the saddle mounts on inside of the frame. And use 10-32 screws to fasten the pitch outer mounting plate to the saddle mounts on outside of the frame (see Figure 15).
15. Use rivets to secure the L-brackets and plate to the frame and inner mounting plate (see Figure 11).
16. Use shims wherever necessary to obtain proper alignment of the hub motors.

Figures 14 and 15 demonstrate what each saddle mount would look like completely assembled and with the frame suppressed from view. Figure 16 displays where each hub will be placed on the inner frame, while Figure 17 shows an up-close view of an attached hub motor to the frame.

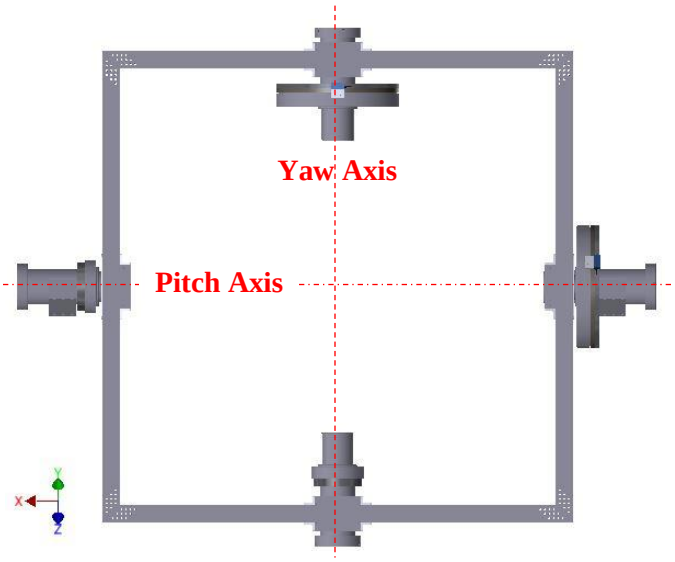

Figure 16: Hub Motors Center Mounted to Inner Frame

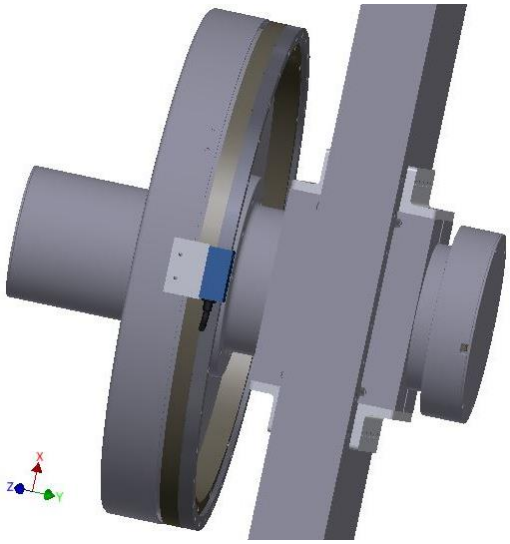

Figure 17: Expanded View of Mounted Hub Motor for Yaw Rotation

Chapter 4

Development of Finite Element Mesh of Inner Frame

FEA Objective

The WASP inner frame model was analyzed using Autodesk Inventor Pro and Abaqus to compare the results from both software applications and obtain an understanding of how the redesigned inner frame would perform in flight-like conditions. To limit the scope of the thesis, FEA was performed on the un-stretched version of the inner frame for deformation simulations due to 10 G loads. A stress analysis was required, under an applied load of 1,500 lbf loading with a factor of safety equal to 10 (15,000 lbf load). The structure must not experience ultimate failure; meaning the structure must not experience an ultimate tensile strength of 45 ksi (refer to Chapter 2: Material Selection).

Details of Assembly

General Approach

The purpose of the WASP frame is to rotate a body—generally an optical telescope—in two axes; 70^{o} in the pitch direction and 15^{o} in the yaw direction. The inner frame was made completely of 6061-T6 aluminum, and had an overall mass of approximately 81 lbm. The assembly was comprised of 14 different parts (see Figures 43 – 56, Appendix B). Reinforcement

plates were positioned wherever there is a cutout or a joint in the frame to strengthen the structure.

Two FEA software packages were utilized because, while Autodesk Inventor Pro is much simpler to use, it is not as accurate as Abaqus. Inventor FEA has severely limited manual input; however, the entire model was able to undergo stress analysis simulations. Abaqus is an extremely powerful FEA software; although it was unable to process the complex geometry of the redesigned WASP inner frame. Therefore, a simplified model of the inner frame, designed in Inventor, was transferred into Abaqus via a STEP file. Once analysis was completed, two probes were placed on the stress plot at two points where the maximum first principal stress occurred along a beam. The average of the two probes provided the resulting first principal stress value used to determine if the frame would fail under the applied load.

Material Properties

6061-T6 aluminum parts were used exclusively for the redesign; its relevant material properties are displayed in Table 2. [9] Inventor inherently knew these properties because each part was specified as 6061-T6 aluminum. However, the properties had to be manually inputted to Abaqus because the material specification was not conveyed to the FEA software when uploaded as a STEP file.

Table 2: Material Properties of 6061-T6 Aluminum

Material Property	Value
Modulus of Elasticity	10,000 ksi
Ultimate Tensile Strength	45 ksi
Tensile Yield Strength	40 ksi
Shear Modulus	3770 ksi
Poisson's Ratio	0.330
Density	0.0975 lb/in^3

The constitutive law that the analysis focused on is the stress-strain constitutive relation for linear materials; the expanded relations are equations (10) – (15) in Appendix C.

External Loading Conditions

Using the Balloon Program specified factor of safety equal to 10, the structure cannot experience ultimate failure under a maximum 15,000 lbf load. The stress analysis was conducted at maximum loading, therefore the WASP inner frame was perpendicular to the outer frame. To shorten runtime, the outer frame was omitted from the FEA. The 15,000 lbf was equally distributed—7,500 lbf on either side of the structure—between two separate center point loads normal to the inner frame (see figures 18 and 19).

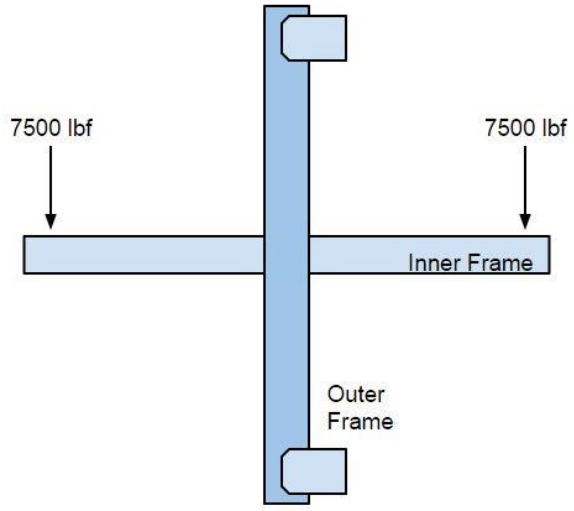

Figure 18: Simplified WASP with Loading

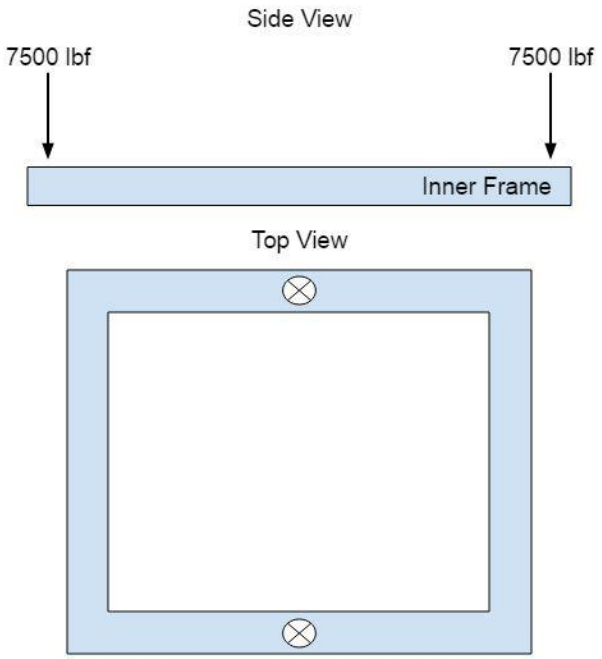

Figure 19: Simplified Inner Frame with Loading

Boundary Conditions and Model Interactions

Inventor Assembly

The main appeal for using Inventor FEA software is that it automatically recognizes and meshes complex geometries for multiple separate parts in one assembly. Unfortunately, the software did not allow the user to manually refine every condition involved in an FEA simulation. Consequently, it was a simplified FEA program. Below are the steps for how a mesh was created, and a static stress analysis was run.

1. Ensure that the material properties were assigned, each part is made from 6061-T6 aluminum.
2. Define constraints: The outer frame should be fixed in place with pins, simulating its attachment to a balloon platform (see Figure 20). The inner frame should be pinned so that it could rotate, but not slip, in the pitch direction—to replicate the motion that will occur with working motors (see Figure 21).

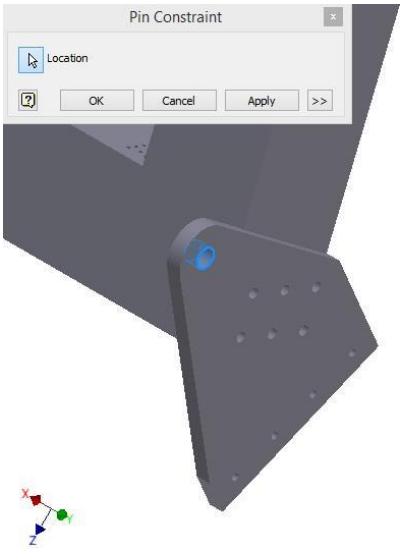

Figure 20: Pin Constraint on Outer Frame Brackets

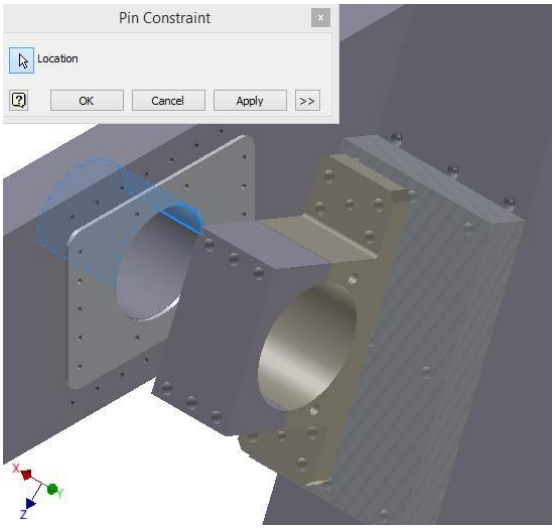

Figure 21: Pin Constraint on Inner Frame Hub Motor Saddle Bracket

3. Use the automatic contact wizard. It intuitively recognized where individual parts connected together in the assembly.
4. Specify the contact in between the two frames as separated with no sliding.

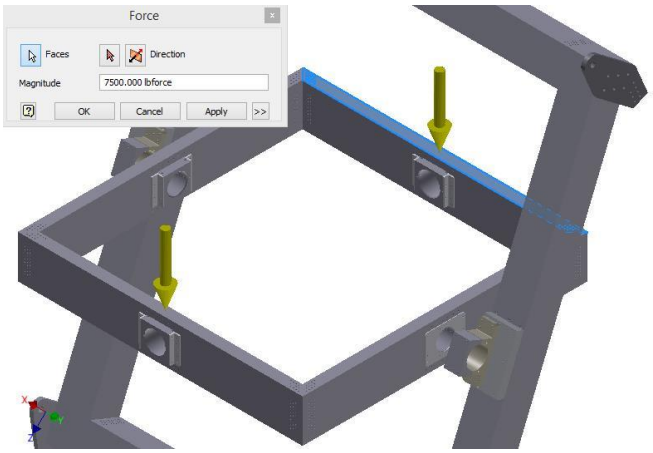

Figure 22: Application of Forces

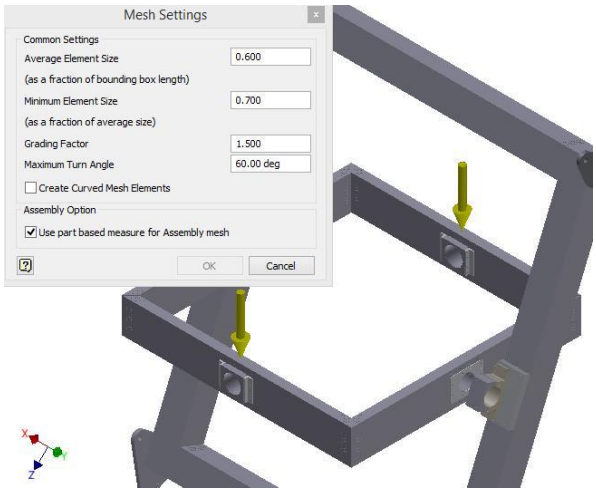

Figure 23: Application of Mesh Settings

5. Apply two concentrated loads of 7,500 lbf on the center of the top surface of the frame, on both yaw beams (see Figure 22).
6. Under Mesh settings set the average element equal to 0.600 in—a medium sized element size—leave all the other settings as default (see Figure 23).

The mesh took about 3-5 minutes to form. The mesh created was not a constant shape or size around any change in geometry (i.e. a hole) or around a

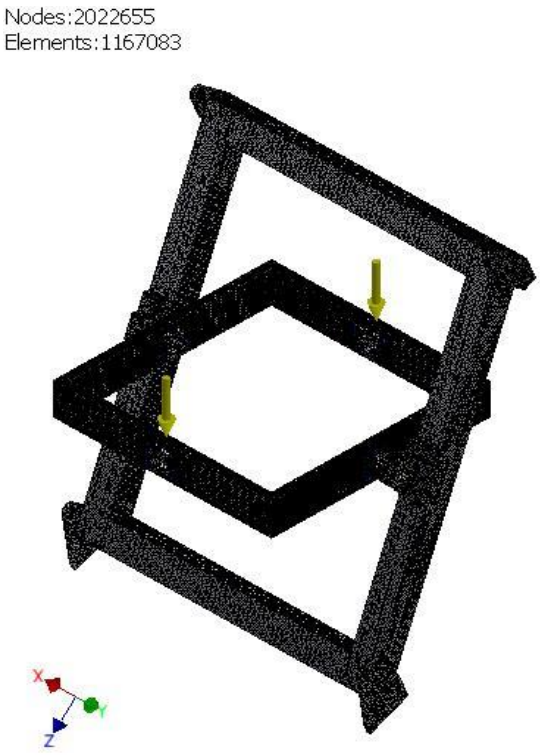

Figure 24: Completed Mesh for WASP Assembly

contact of another part which is indicative of a poor quality mesh (sees Figures 24 – 26). Unfortunately, Inventor did not allow the user to select the shape of the mesh—tets, bricks, prisms, or pyramids—nor did it provide the option to apply mesh controls around changes in geometry/part interactions.

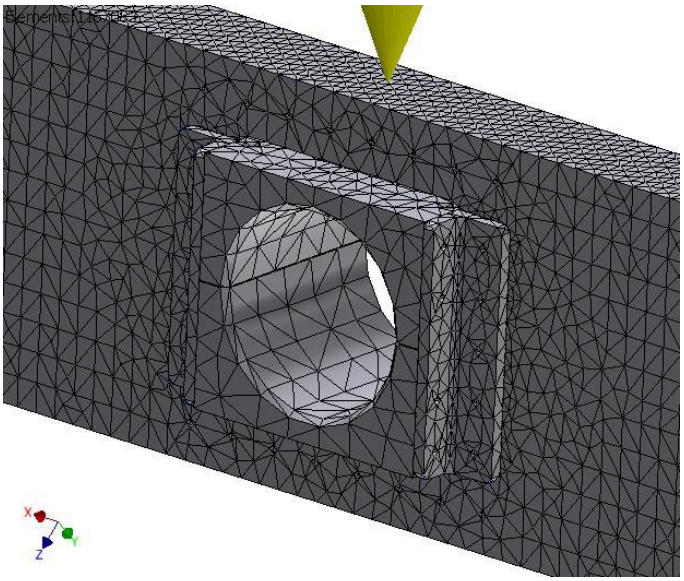

Figure 25: Close-up View of Hub Motor Saddle Mount

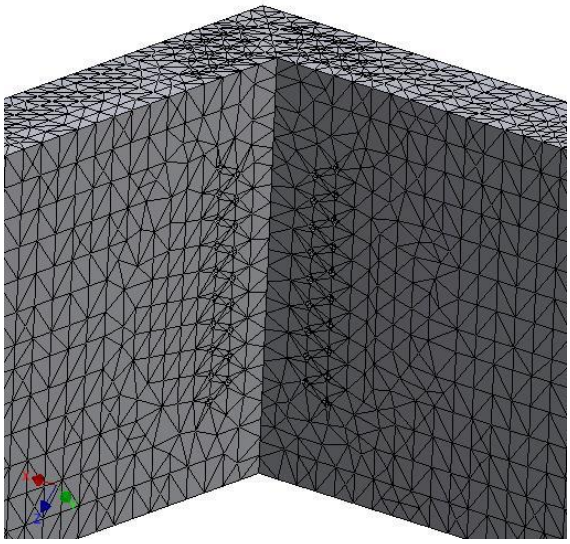

Figure 26: Close-up View of Inner Frame Corner Joint

Abaqus Assembly

Error messages occurred continually while importing the entire WASP assembly as single and multiple parts into Abaqus. The program could not handle complex geometries, such as fillets. Therefore, a simplified representation of the inner frame was made and the model was imported from Autodesk Inventor into Abaqus as a STEP file. Below are the steps for how a mesh was created, and a static stress analysis was run.

1. Designate density under the Property Tab.

2. Assign Young's modulus and Poisson's ratio in the Mechanical Elastic Properties section.
3. Create a homogenous solid section assigned to the frame.
4. Under the Step Tab, create a "Static, General" step with an initial incremental size of 1; with a minimum increment size of $1x10^{-5}$ and maximum increment size of 1.
5. Select the element shape as tet (a triangle type element) and assign the mesh over the whole frame.

The mesh was of high quality because all the elements were roughly the same size and shape (see Figure 27). However, the mesh was applied to an extremely simplified design of the WASP frame, and hence would not produce an accurate representation of deformation at a 10 G load.

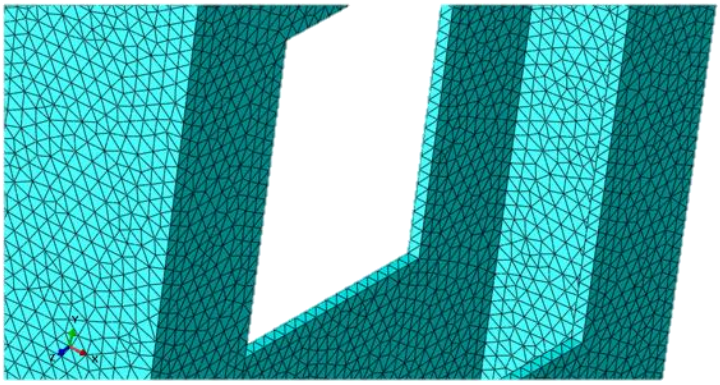

Figure 27: Close-up View of Initial Mesh on Simplified Inner Frame in Abaqus

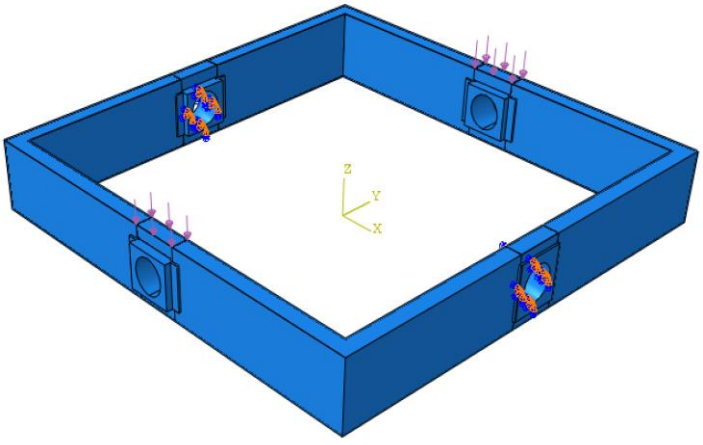

Figure 28: Applied Load and Boundary Conditions to Simplified Inner Frame

A new solid body model which more closely resembled the inner frame—yet still omitted complex geometry features, such as fillets—was designed in Autodesk Inventor Pro and imported into Abaqus. The 7,500 lbf per side was distributed over an individual

area of 0.01 in^2, to concentrate the applied load. Displacement and rotational boundary conditions were applied to the pitch-axis mounting holes (see Figure 28).

Three iterations were conducted in Abaqus to further refine the mesh prior to analysis with the aim of obtaining accurate and converging results. Table 8 in Appendix A displays the meshing settings and controls used on the WASP frame as well as the time required to create the mesh. Time taken to assemble the mesh increased with each iteration, mainly because the global mesh element size decreased each time. Mesh controls were also implemented in regions of high stress concentrations; the controls were tightened with each iteration. Figure 29 illustrates the mesh conditions applied to a joint of the frame during the second iteration. Figure 30 displays the mesh controls applied to the high concentration stress area around a hub mount during the third iteration.

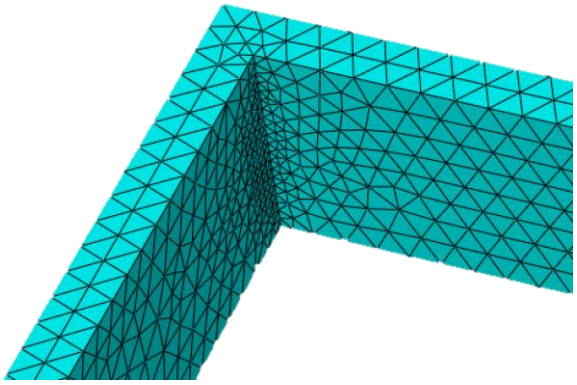

Figure 29: Application of Mesh Control in Corner of Frame, 2nd Iteration

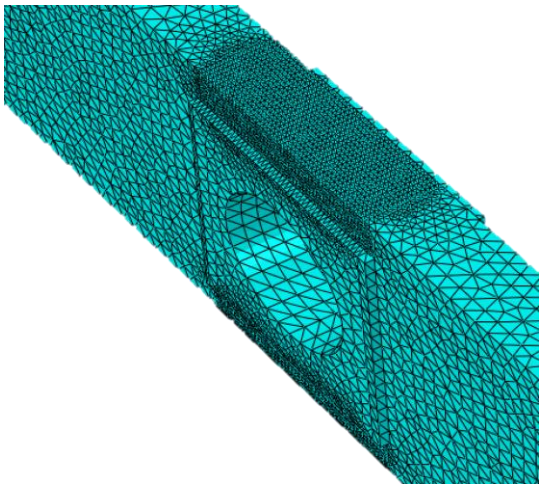

Figure 30: Application of Mesh Control in High Stress Area, 3rd Iteration

The 3rd, and final, iteration of the mesh resulted in a global mesh size of 0.39 in, a mesh control of 0.39 in at the frame joints, a mesh control in high stress concentration areas of 0.12 in

(see Figure 31), and a total run time of 18.78s to create. The reduced global size and mesh control sizes resulted in a much higher quality mesh.

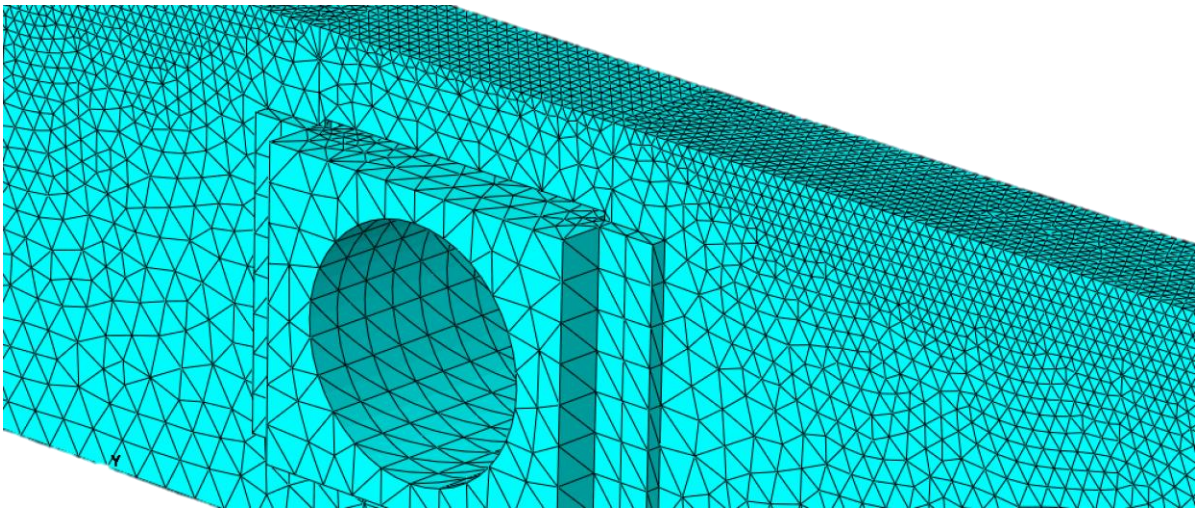

Figure 31: Expanded View of Final Mesh, 3rd Iteration

Chapter 5

Analysis of Finite Element Model

Inventor Finite Element Analysis Results

Autodesk Inventor Pro FEA package was extremely intuitive and easy to use, although it severely limits options available to the user to improve mesh settings. The software runs the mesh and analysis/simulation automatically. The simulation completed in approximately 17 minutes, which was a relatively short run time. Obtaining FEA simulations often requires substantial amounts of computer processing and time.

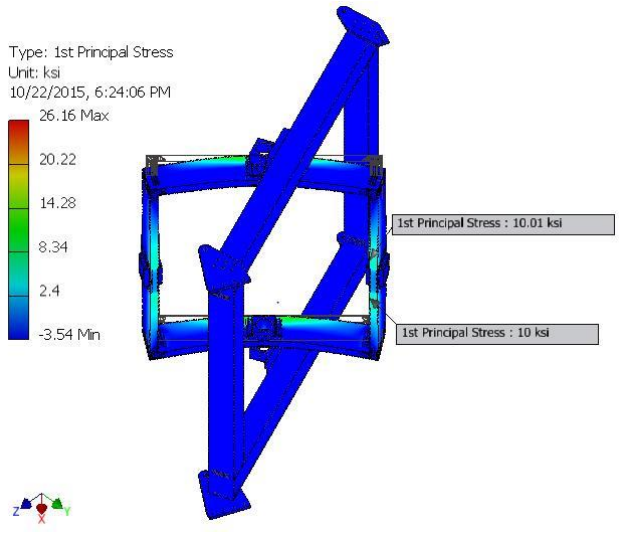

Figure 32: First Principal Stress Plot

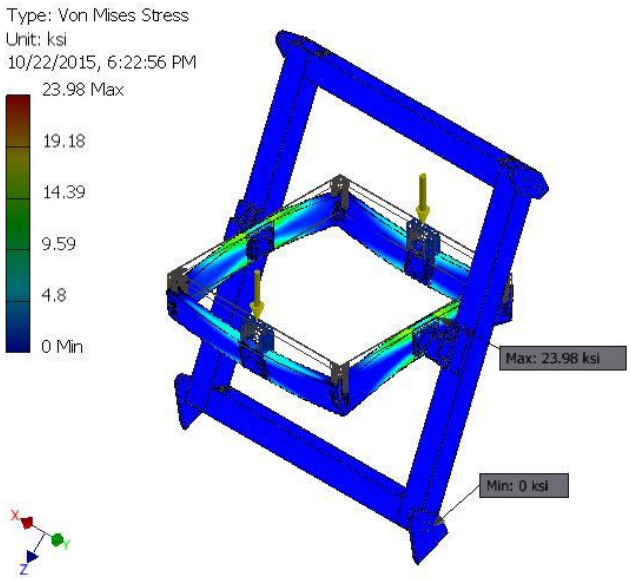

Figure 33: Von Mises Stress Plot

Figure 32 portrays the First Principal stress results. Two probes were placed where the maximum stress was expected to occur (refer back to Chapter 2: Theoretical Analysis). The

average of the sum of those two probes was about 10 ksi. The simple hand calculation of a center-loaded beam provided a maximum principal stress of approximately 11.4 ksi (refer to Chapter 2: Theoretical Analysis and see Table 7, Appendix A). The percent difference between the Inventor FEA and the hand calculation is approximately 13.5%. The discrepancy might be due in part to the large element size and un-uniform element shape/pattern; which occurred because Inventor does not allow the user to choose those functions manually. However, the difference may also be due in part to the use of simplifying the frame to a center-loaded beam to model the stress by hand. The Von Mises stress was used to predict yielding of the assembly; if the structure reached the material yield strength, the structure would undergo yielding. Figure 33 depicts the Von Mises stress results; the maximum value was about 24 ksi. The most important take away from the FEA results was that both the maximum Von Mises and First Principal stress were significantly lower than the UTS, 45 ksi, and yielding stress, 40 ksi, for an 6061-T6 aluminum structure. Thus, the lighter version of WASP would not experience ultimate failure.

Abaqus Finite Element Analysis Results

Abaqus was an extremely powerful FEA software, but it could not process the imported complete assembly of the inner frame due to its complex geometries. Hence, simulations were conducted on a simplified version of the inner frame and the results converged after three iterations. The final iteration analysis completed in 19:40 minutes; which was a relatively short run time, but longer than the previous iterations mainly because the mesh resolution was much greater. High stress concentrations occurred at all the corners and pivot holes for the simplified frame. This demonstrated that the reinforcement plates and geometry features—such as fillets,

which increase strength in high stress areas—included in the redesigned version of WASP were necessary to the integrity of the design, and therefore cannot be removed to save weight. Thus, the abnormally high stresses in those areas were ignored in the analysis because they were not a true representation of what the real frame would experience.

Figure 34 depicts the First Principal stress results. The maximum principal stresses occurred around each corner of the center mounts on the simplified frame model. These were much higher than the stresses that occurred on the redesigned WASP inner frame, because the simplified model did not include the reinforcement plates and geometry features to counteract stress concentrating at the corners. However, the high stress area was close enough to the predicted position of the maximum stress that the area was considered in the analysis. The first principal stress was averaged over patch of six nodes, which found a maximum of approximately 11.2 ksi. The percent difference between the Abaqus FEA and the hand calculation was about 2.4%. The major reason why Abaqus has a small percent difference is that an over-simplified geometry was used, which more closely resembles a simple center-loaded beam. The Von Mises stresses were analyzed at the same cluster of 6 nodes (see Figure 35), which found a maximum of approximately 10.7 ksi. Both of these values are significantly lower than the UTS, 45 ksi, and yielding stress, 40 ksi, for an 6061-T6 aluminum structure. Thus, the simplified version of the inner frame would not experience ultimate failure.

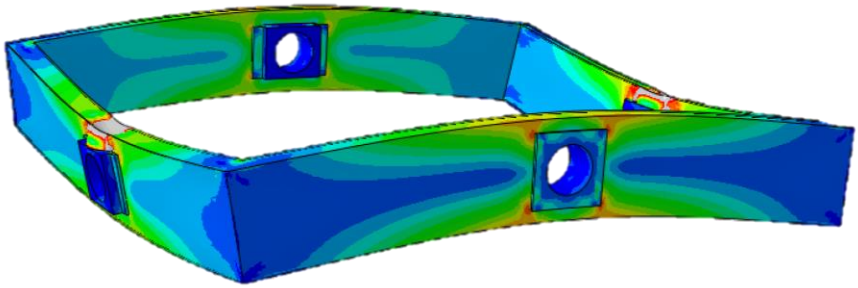

Figure 34: First Principal Stress Plot on the Simplistic Model of Inner Frame

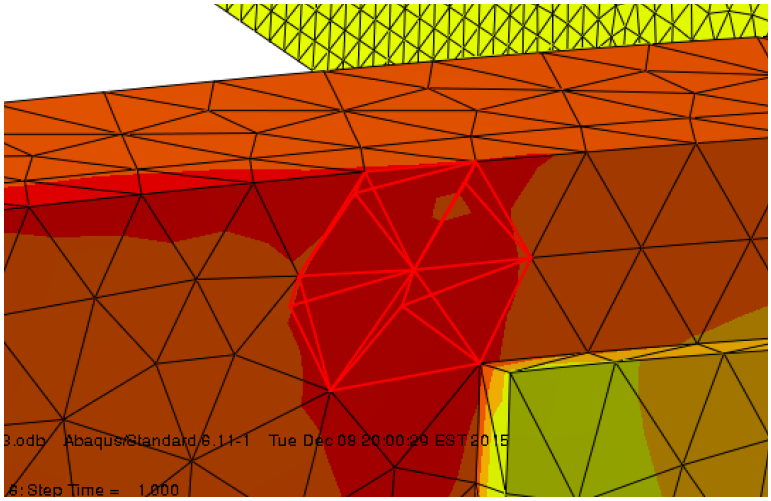

Figure 35: Von Mises Stress Plot of Simplistic Frame

Figures 38 – 40 in Appendix B display the linear relationship between principal stress vs. time, principal strain vs. time, and Von Mises vs. time. Several nodes were manually selected in the area of high stress concentrations to analyze the maximum stress and strain along the path (see Figures 41 and 42, Appendix B). Figure 36 displays the path chosen for analysis.

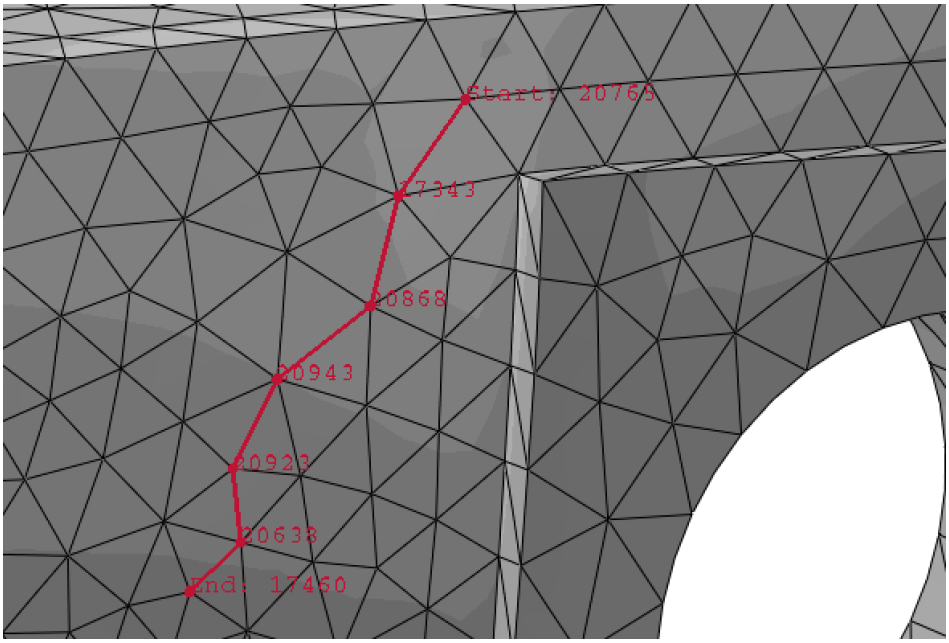

Figure 36: Stress Path Plotted in High Stress Area

Chapter 6

Conclusion

The purpose for redesigning the WASP structure was to reduce the weight by at least 100 lbm, about 18% lighter than the original, while maintaining the stiffness and strength of the original design. The redesigned un-stretched version of WASP (see Figure 37) is 161 lbm, or 31% lighter than the original design. Additionally, a stretched version of the inner frame was designed to provide greater flexibility to prospective payloads; the resulting weight was 156, or approximately 30% lighter than the original. The strength and stiffness were minimally impacted, but not significant enough to cause ultimate failure. FEA was conducted using Autodesk Inventor Pro and Abaqus. While Inventor resulted in a 13.5% difference and Abaqus produced a 2.4% difference from the theoretical calculations for maximum stress on a beam, both simulations demonstrated that the structure would not experience stresses close to the material UTS and yield strength. Additionally,

Figure 37: Redesigned WASP Assembly

the redesigned version utilized standard off-the-shelf extrusions for the inner frame to maintain cost-effectiveness.

Future FEA simulations that could be of interest include, but are not limited to: a modal test, steady state thermal test, and a transient thermal test. Balloons typically do not experience significant vibration during flight, thus a modal test would ensure that the structure resonates at a frequency far outside a low frequency of 20 Hz—a general Balloon Program Standard. The steady state thermal test would verify that each component eventually cools from 80^{o}C to -90^{o}C—a general Balloon Program Standard. The transient thermal test would assess the time to cool each component from 80^{o}C to -90^{o}C.

The redesigned WASP met all of the project requirements. Thus, the NASA Mechanical Systems Branch engineers and technician approved the structure.

Appendix A

Appendix of Tables

Table 3: Honeycomb Calculations

Face Material = 6061 T6			Core Material = 5056			b (in)	2.00
	MPa	psi		MPa	psi	l (in	53.25
Yield Strength	240	34809.12	Ec Modulus	669	97030.42	tc (in)	4.00
Ef Modulus	70	10152.66	Longitudinal Shear	1.7	246.5646	tf (in)	0.020
Poisson	0.33	0.33	GL Modulus	310	44961.78	P (lbf)	7500.00
			Traverse Shear	1.1	159.5418	kb	0.021
			GW Modulus	138	20015.24	ks	0.25
			Stabilized Compression	2.4	348.0912	h (in)	4.02
						D (N*in^2)	3229.24
						S (N)	160910.00
						Bend (lbf*in)	49921.88
						Shear (lbf)	3750.00

Deflection Bend (in)	7305.98
Deflection Shear (in)	0.62

Deflection Total (in)	7306.60
Facing Stress (psi)	315451.32
Core Stress (psi)	466.45

Table 4: Beam Deflection and Stress Calculations Original at 1G

E (ksi)	Weight (lb)	*l* (in)	c (in)	Disp at x (in)	Moment_ max (lb*in)	Stress_max (psi)	Shear_max (lb)
10000.00	750.00	53.25	2.50	0.026	9984.38	696.79	375.00
		62.50	2.50	0.043	11718.75	817.82	

		% Diff @ *l* = 53.25	% Diff @ *l* = 62.5	Margin @ l = 53.25	Margin @ l = 62.5
Tensile Yielding Strength (psi)	40000	193.15	191.99	56.41	47.91
Ultimate Tensile Strength (psi)	45000	193.90	192.86	63.58	54.02

Table 5: Beam Deflection and Stress Calculations Original at 10G

E (ksi)	Weight (lb)	*l* (in)	c (in)	Disp at x (in)	Moment_ max (lb*in)	Stress_max (psi)	Shear_max (lb)
10000.00	7500.00	53.25	2.50	0.263	99843.75	6967.87	3750.00
		62.50	2.50	0.426	117187.50	8178.25	

		% Diff @ *l* = 53.25	% Diff @ *l* = 62.5	Margin @ l = 53.25	Margin @ l = 62.5
Tensile Yielding Strength (psi)	40000	140.66	132.10	4.74	3.89
Ultimate Tensile Strength (psi)	45000	146.37	138.48	5.46	4.50

Table 6: Beam Deflection and Stress Calculations 8x2x0.125 at 1G

E (ksi)	Weight (lb)	*l* (in)	c (in)	Disp at x (in)	Moment_ max (lb*in)	Stress_max (psi)	Shear_max (lb)
10000.00	750.00	53.25	4.00	0.027	9984.38	1144.33	375.00
		62.50	4.00	0.044	11718.75	1343.11	

		% Diff @ *l* = 53.25	% Diff @ *l* = 62.5	Margin @ l = 53.25	Margin @ l = 62.5
Tensile Yielding Strength (psi)	40000	188.87	187.01	33.96	28.78
Ultimate Tensile Strength (psi)	45000	190.08	188.41	38.32	32.50

Table 7: Beam Deflection and Stress Calculations 8x2x0.125 at 10G

E (ksi)	Weight (lb)	*l* (in)	c (in)	Disp at x (in)	Moment_ max (lb*in)	Stress_max (psi)	Shear_max (lb)
10000.00	7500.00	53.25	4.00	0.270	99843.75	11443.28	3750.00
		62.50	4.00	0.437	117187.50	13431.08	

		% Diff @ *l* = 53.25	% Diff @ *l* = 62.5	Margin @ l = 53.25	Margin @ l = 62.5
Tensile Yielding Strength (psi)	40000	111.02	99.45	2.50	1.98
Ultimate Tensile Strength (psi)	45000	118.90	108.06	2.93	2.35

Table 8: Abaqus Mesh and Run Data

Mesh Run	1	2	3
Mesh Time (s)	4.53	6.98	18.78
Run Time (s)	17.82	01:05.6	03:26.7
Global Size (in)	1.18	0.79	0.39
Mesh Control (in) at Corners	0.39	0.39	0.39
Mesh Control (in) at High Stress Points	N/A	0.20	0.12

Appendix B

Appendix of Figures

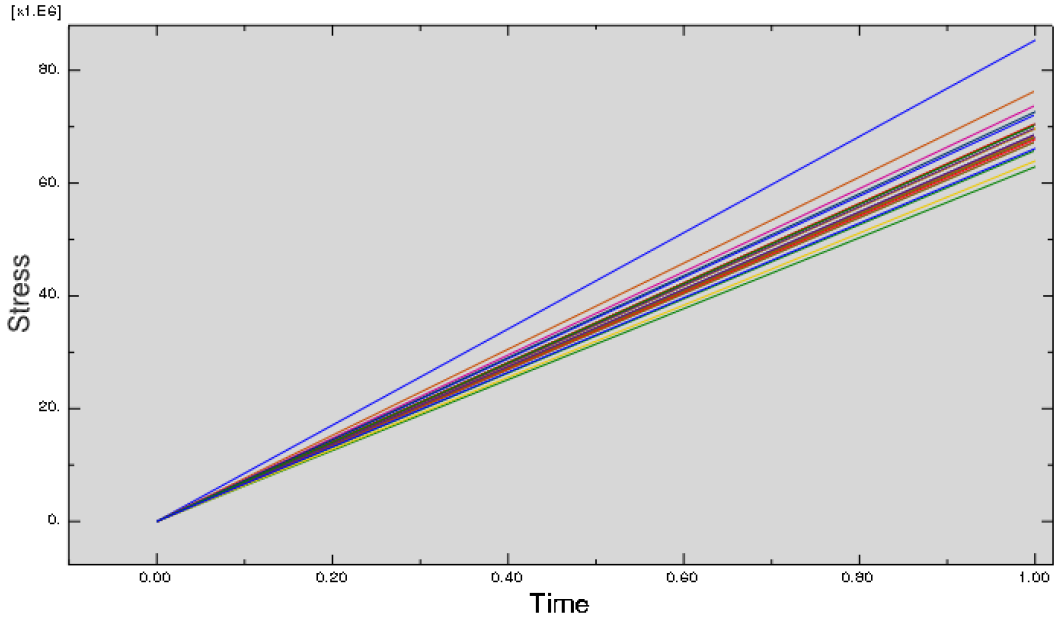

Figure 38: Principal Stress vs. Time

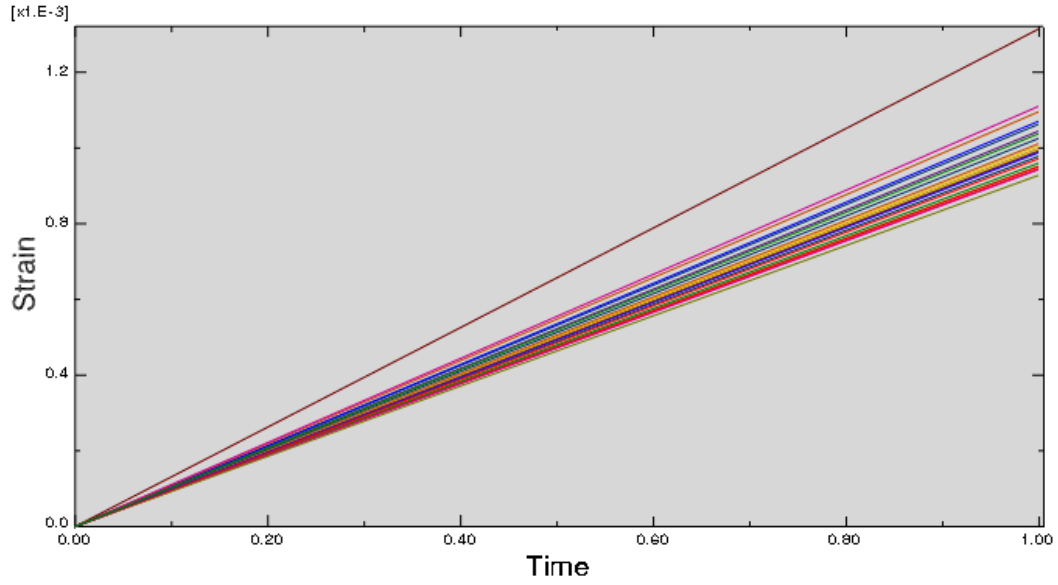

Figure 39: Principal Strain vs. Time

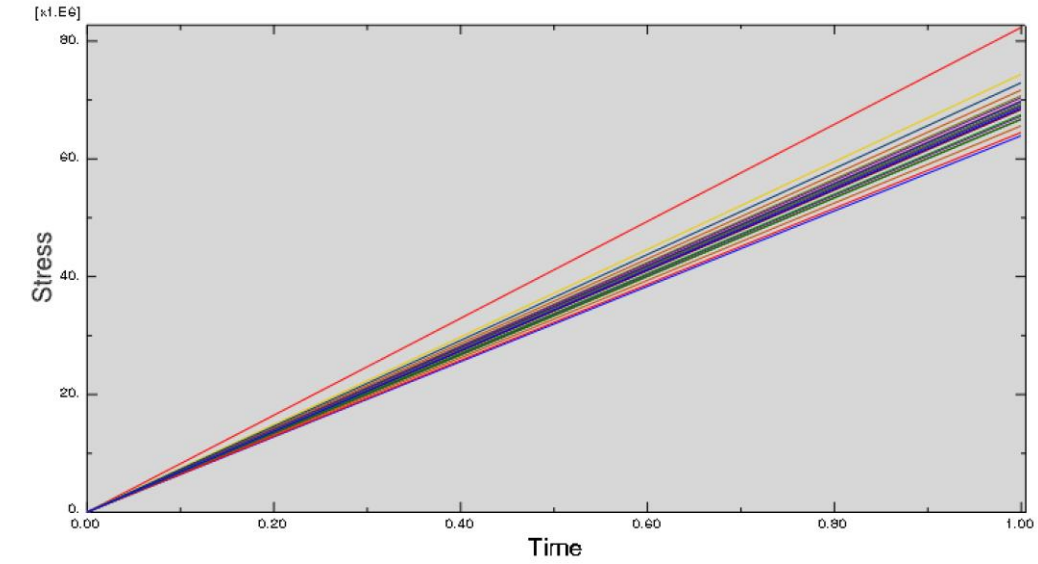

Figure 40: Von Mises Stress vs. Time

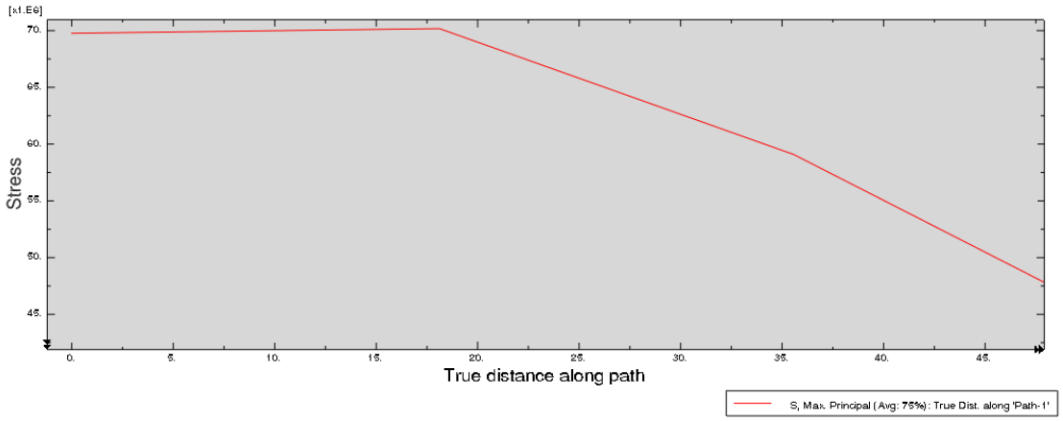

Figure 41: Max Principal Stress Along a Path

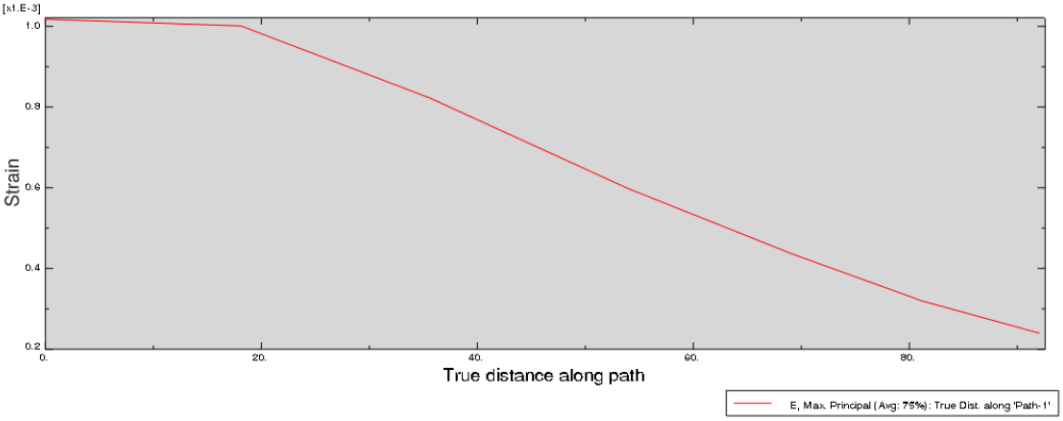

Figure 42: Max Principal Strain Along a Path

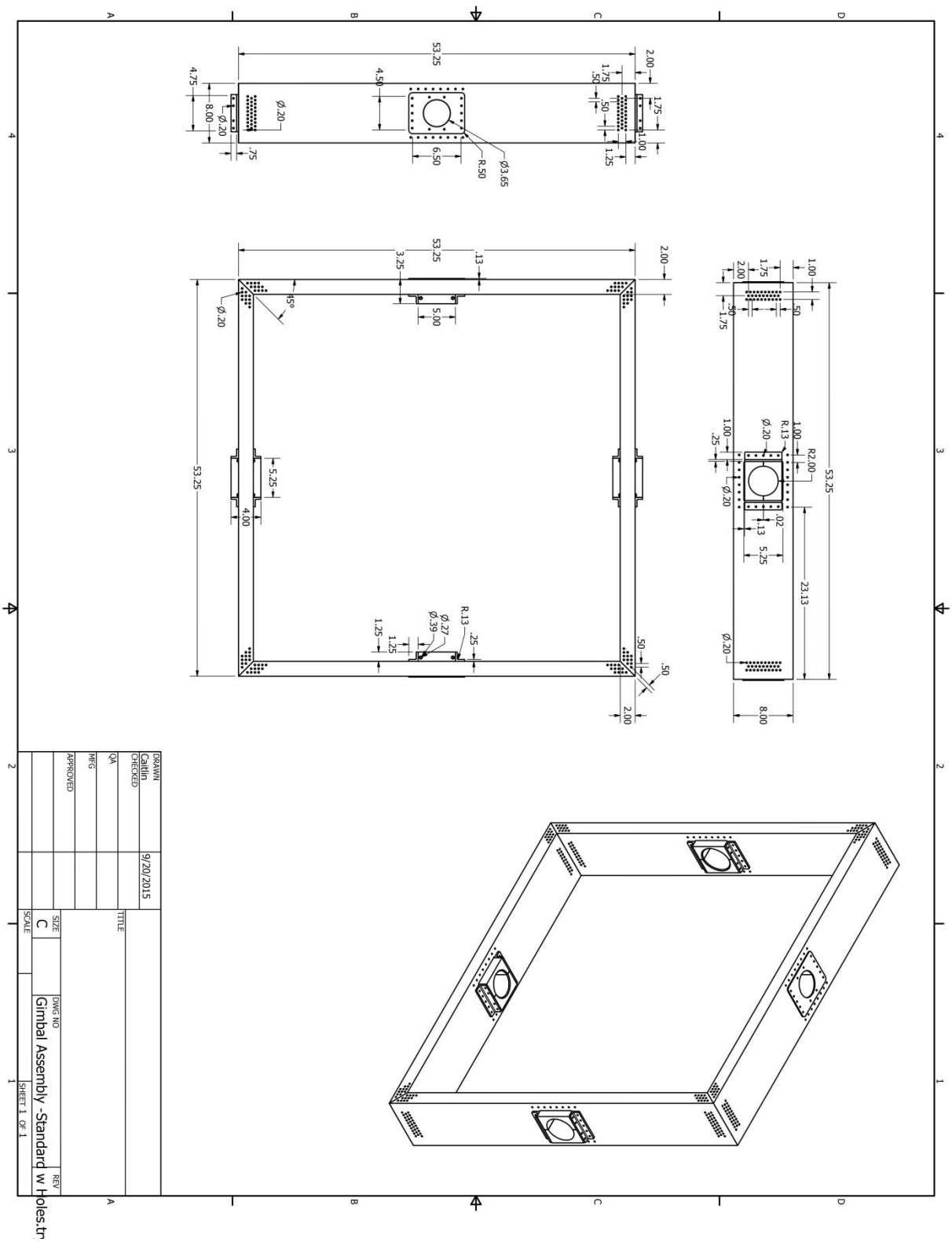

Figure 43: CAD Drawings of WASP Inner Frame Assembly

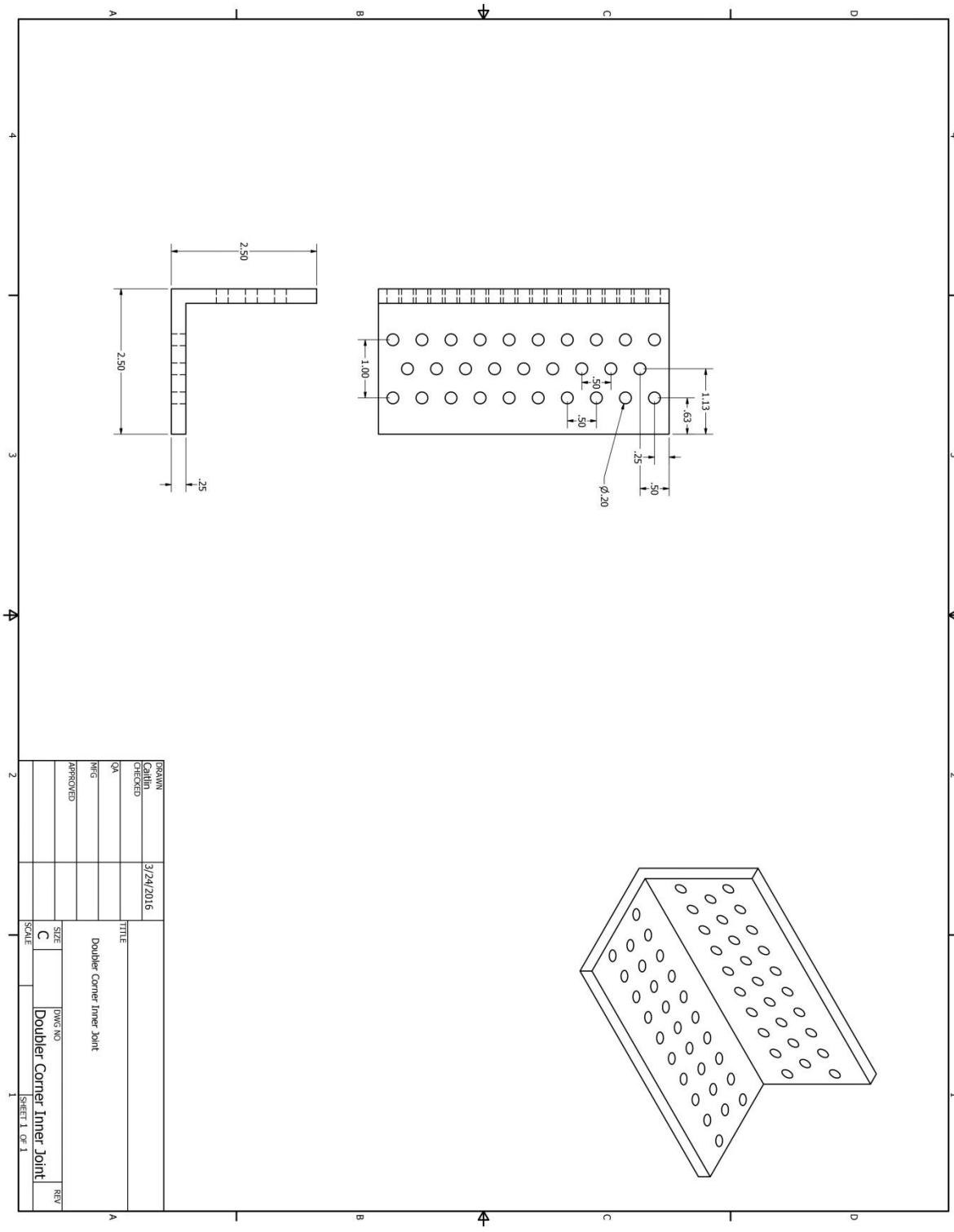

Figure 44: Doubler Corner Inner Bracket

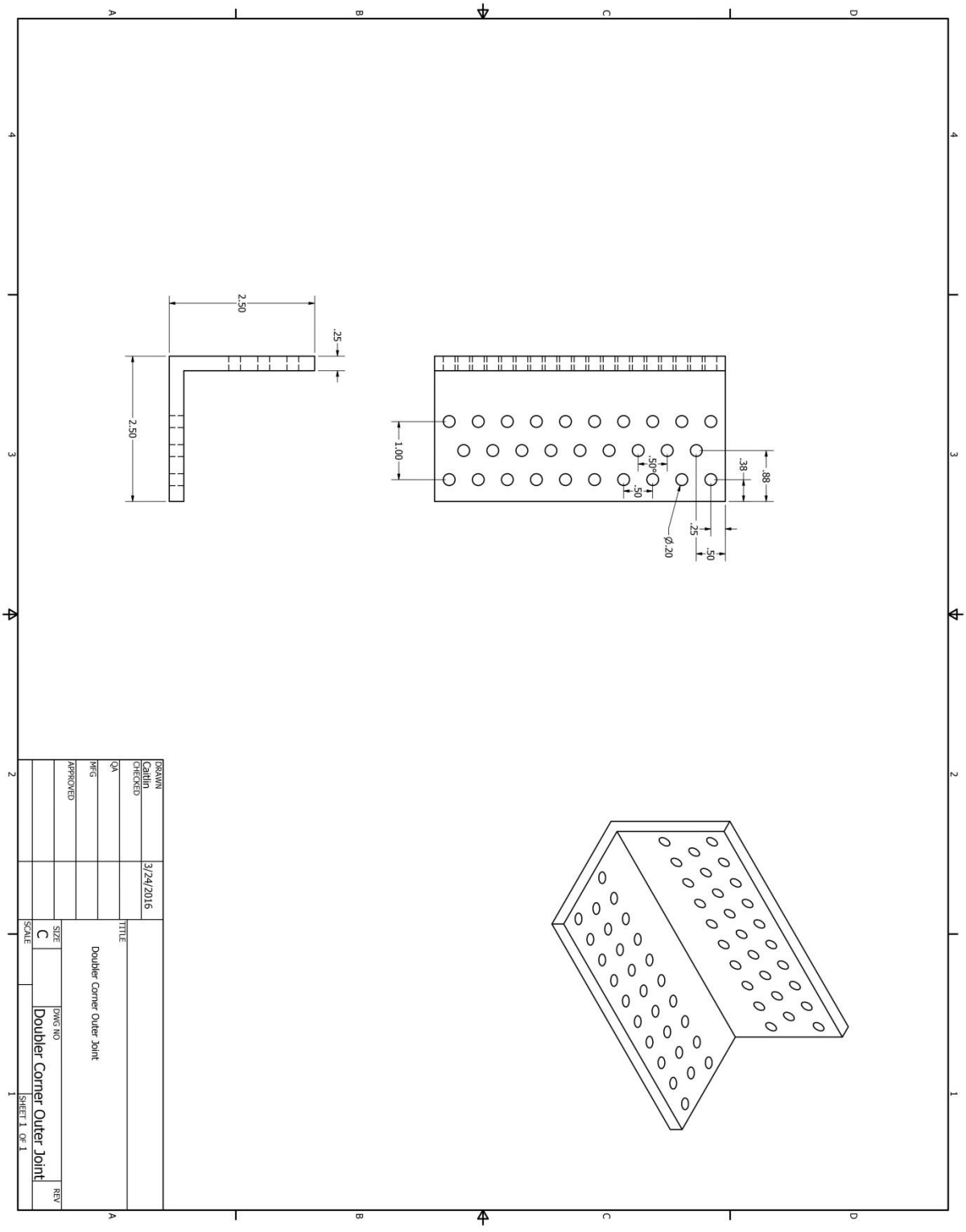

Figure 45: Doubler Corner Outer Bracket

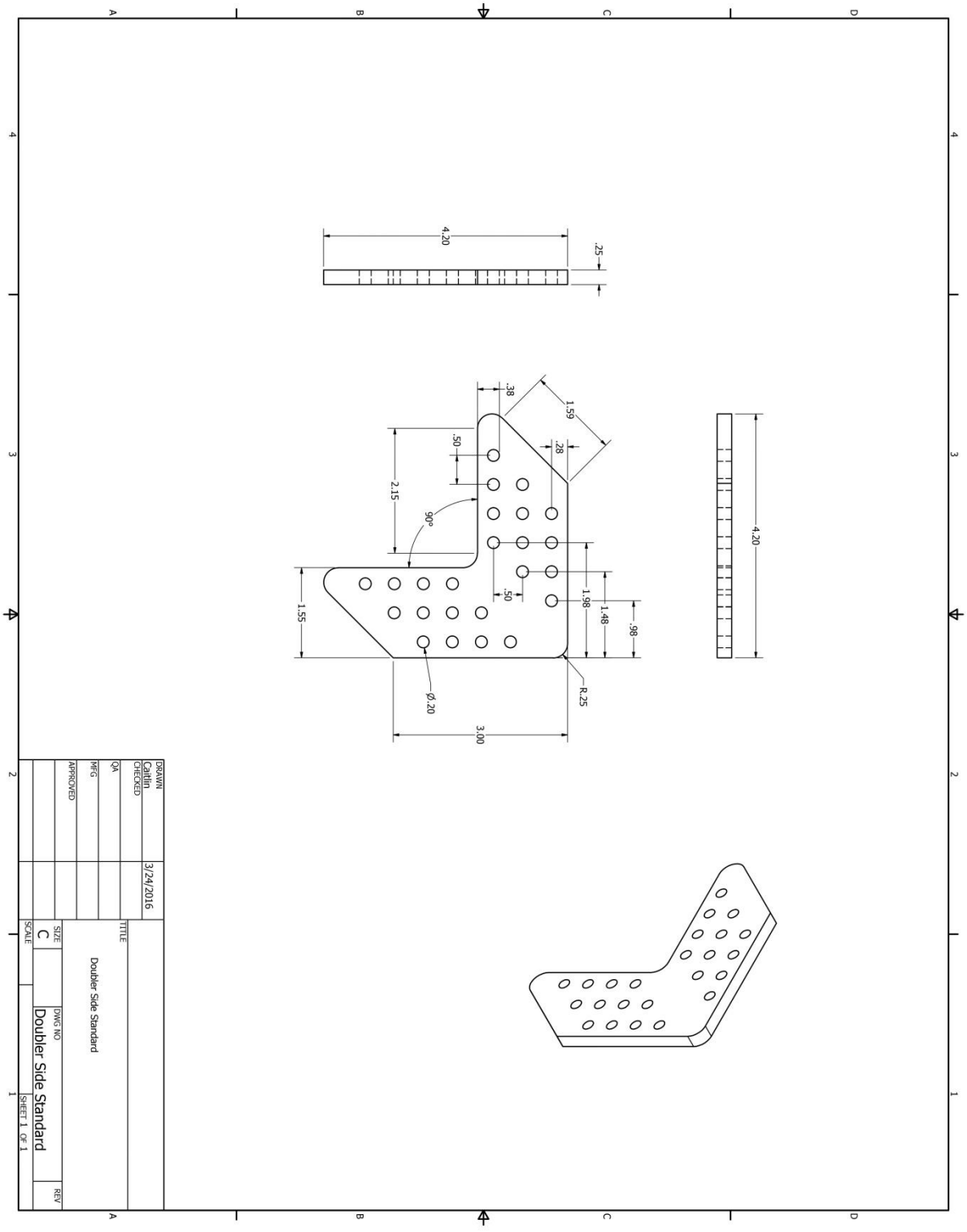

Figure 46: Doubler Side Standard

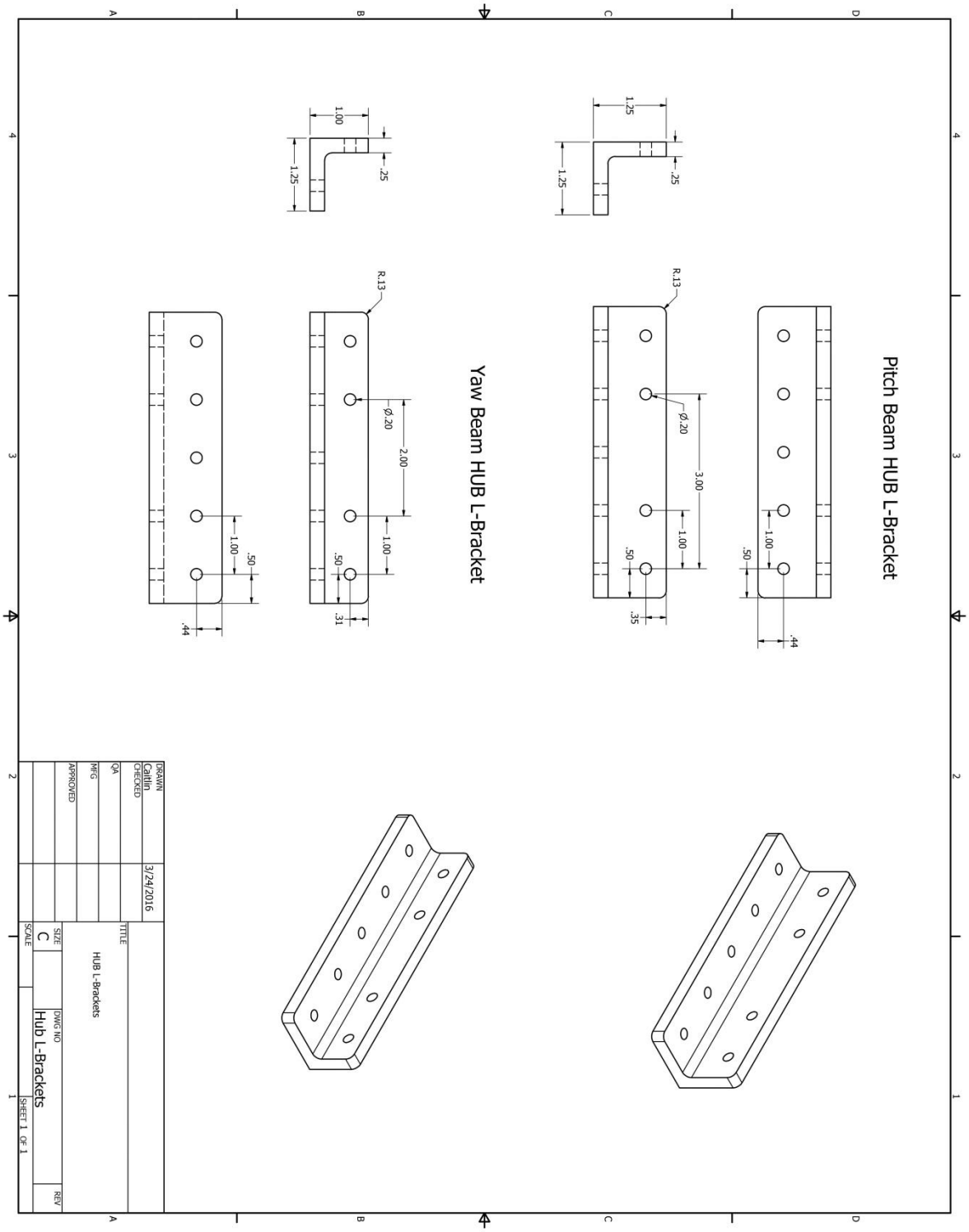

Figure 47: Hub L-Brackets

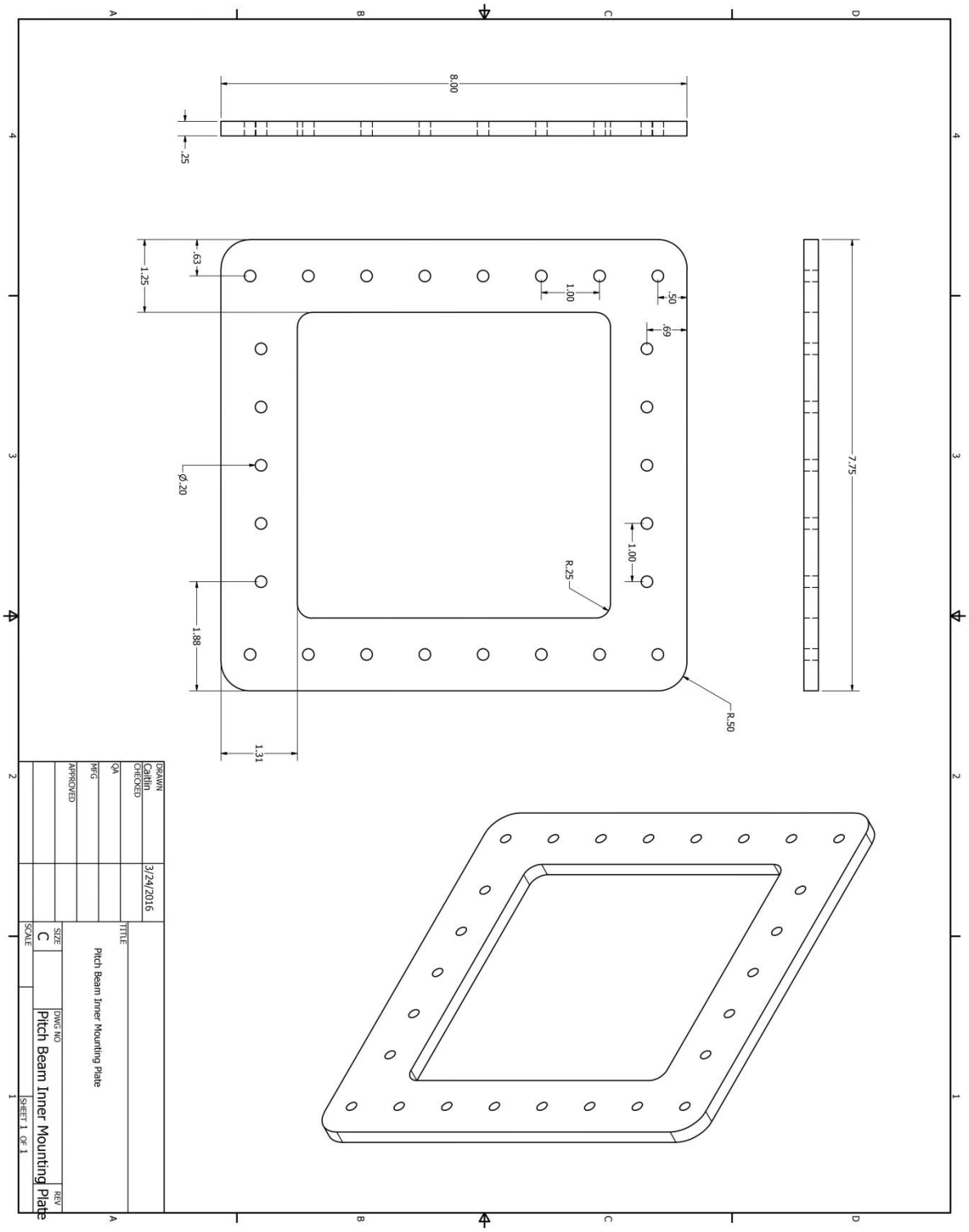

Figure 48: Pitch Inner Mounting Plate

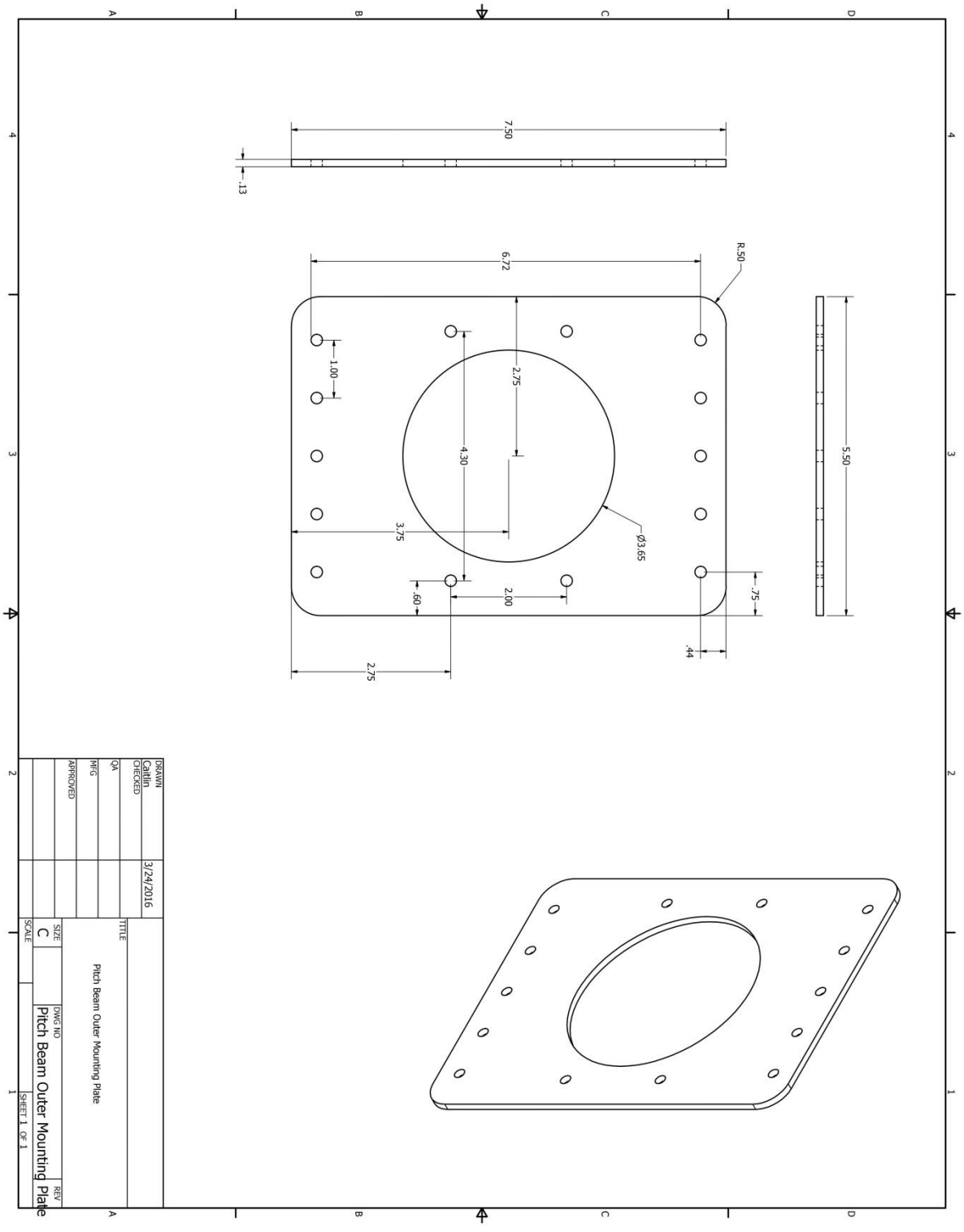

Figure 49: Pitch Outer Mounting Plate

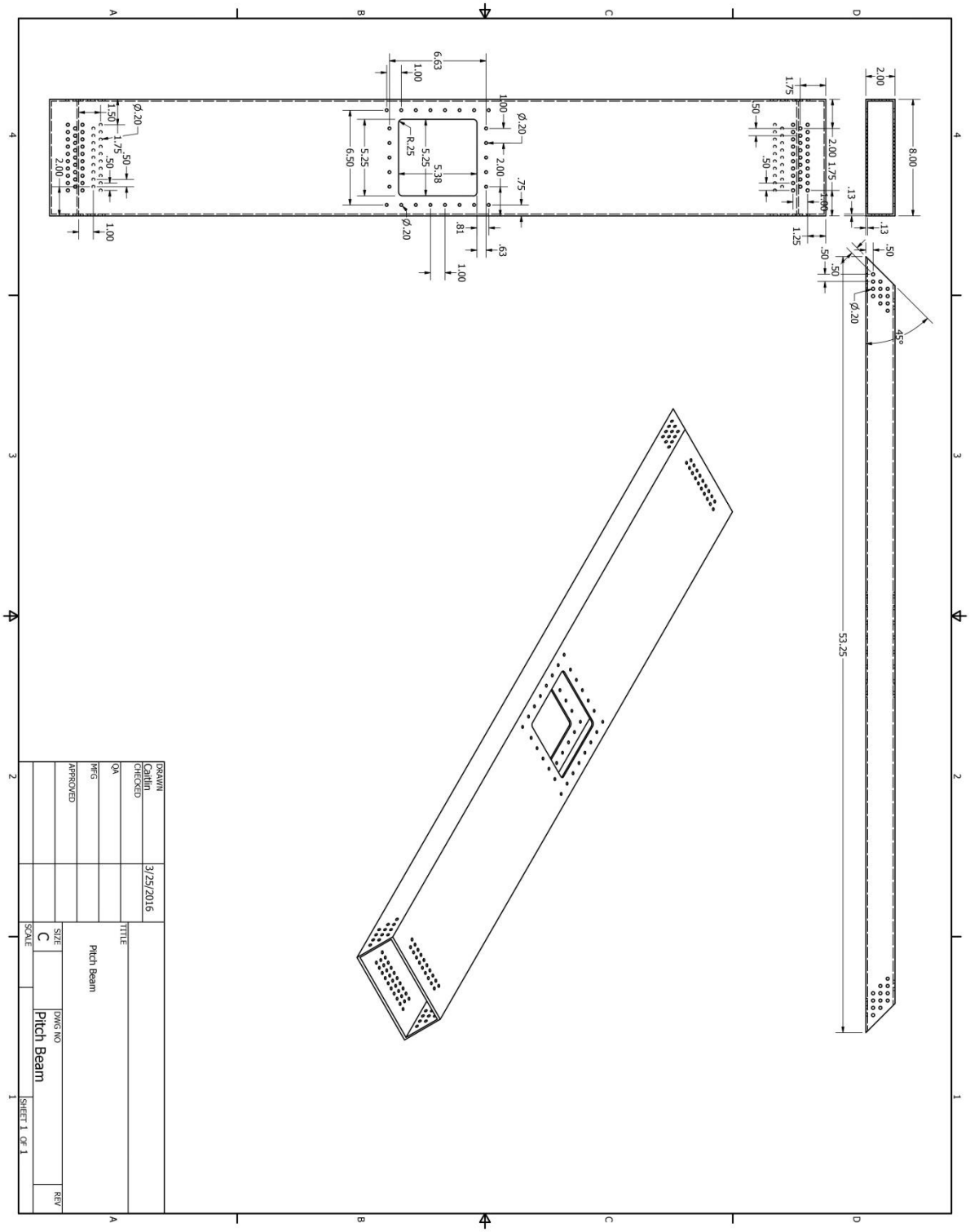

Figure 50: Pitch Beam

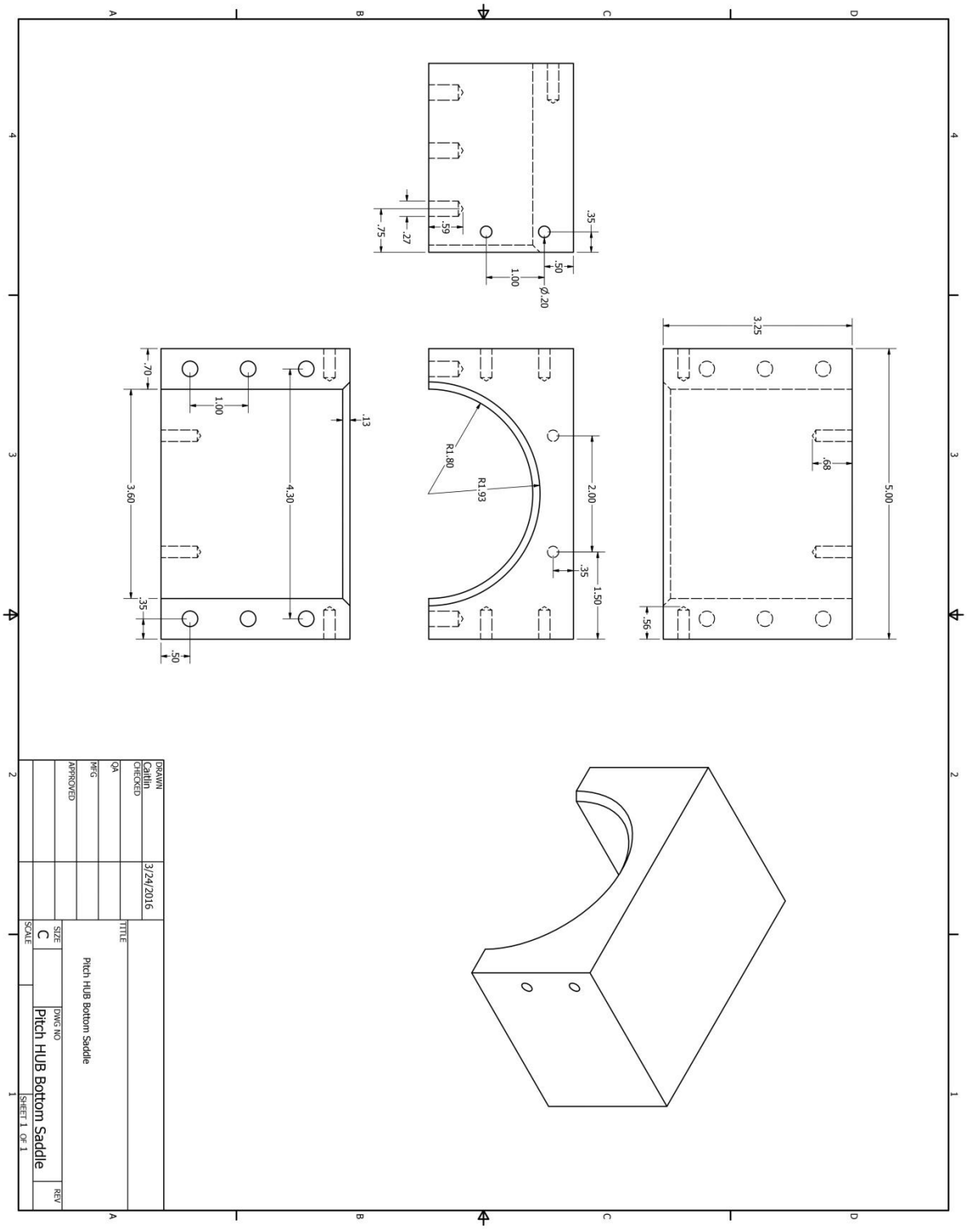

Figure 51: Pitch Hub Bottom Saddle Mount

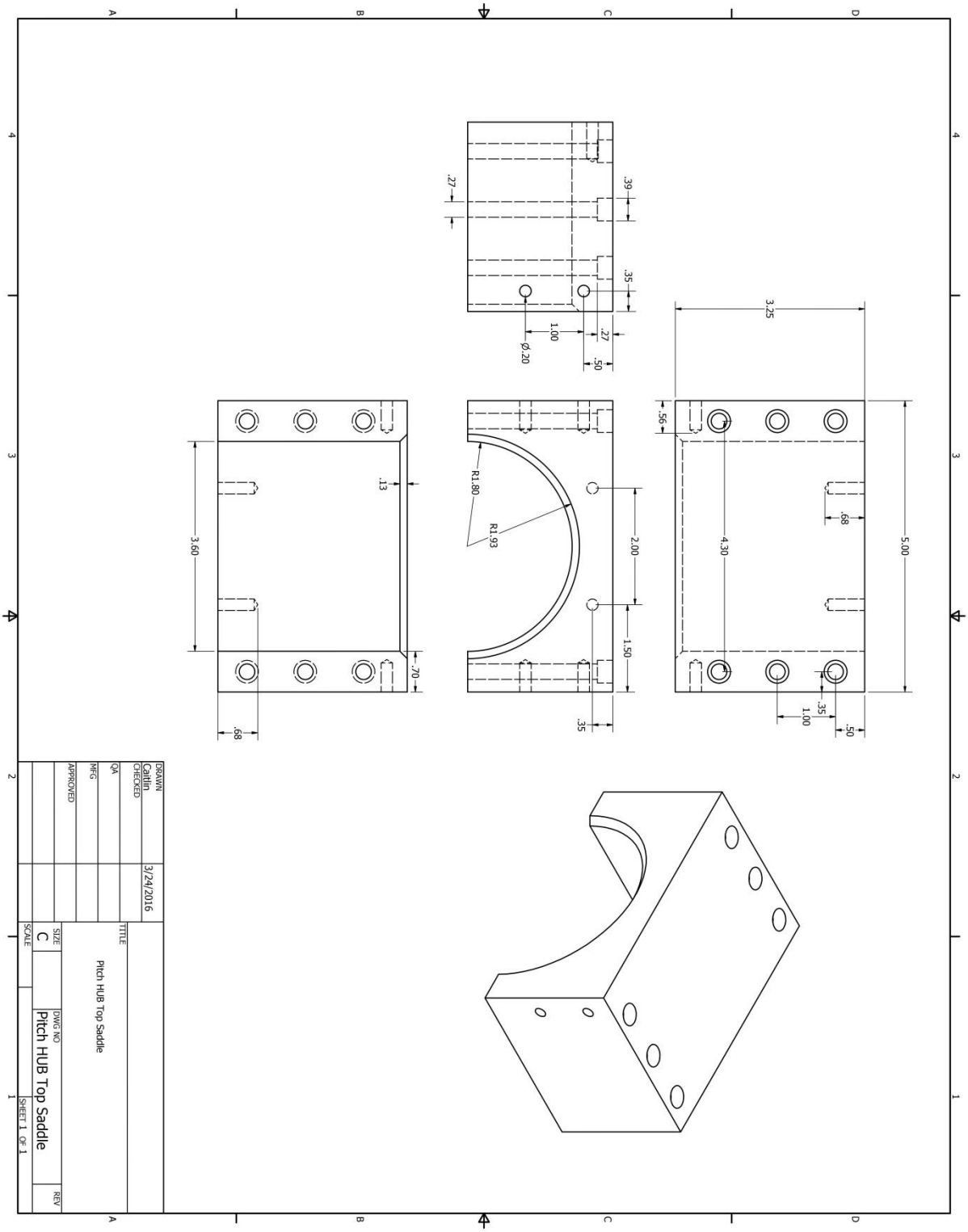

Figure 52: Pitch Hub Top Saddle Mount

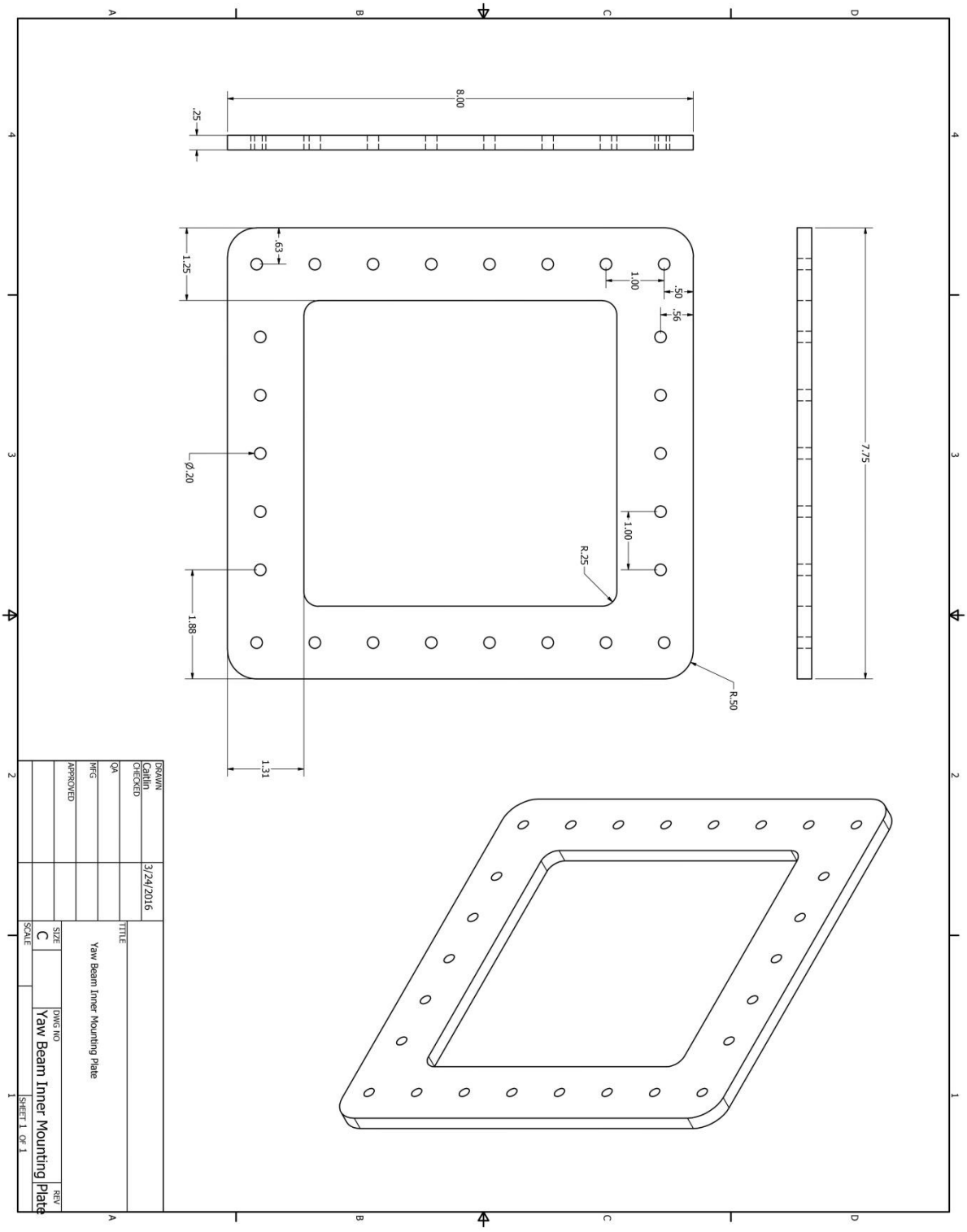

Figure 53: Yaw Inner Mounting Plate

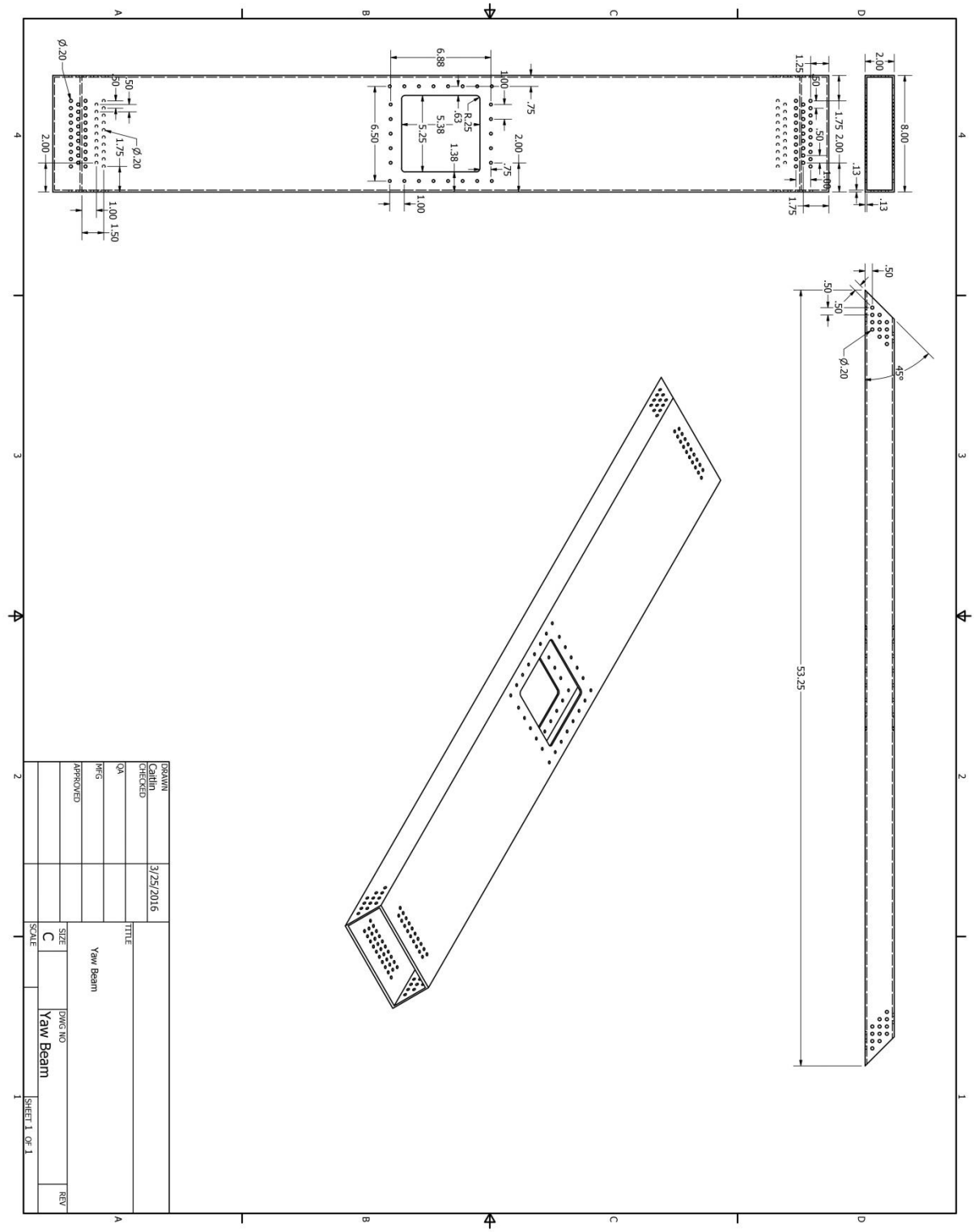

Figure 54: Yaw Beam

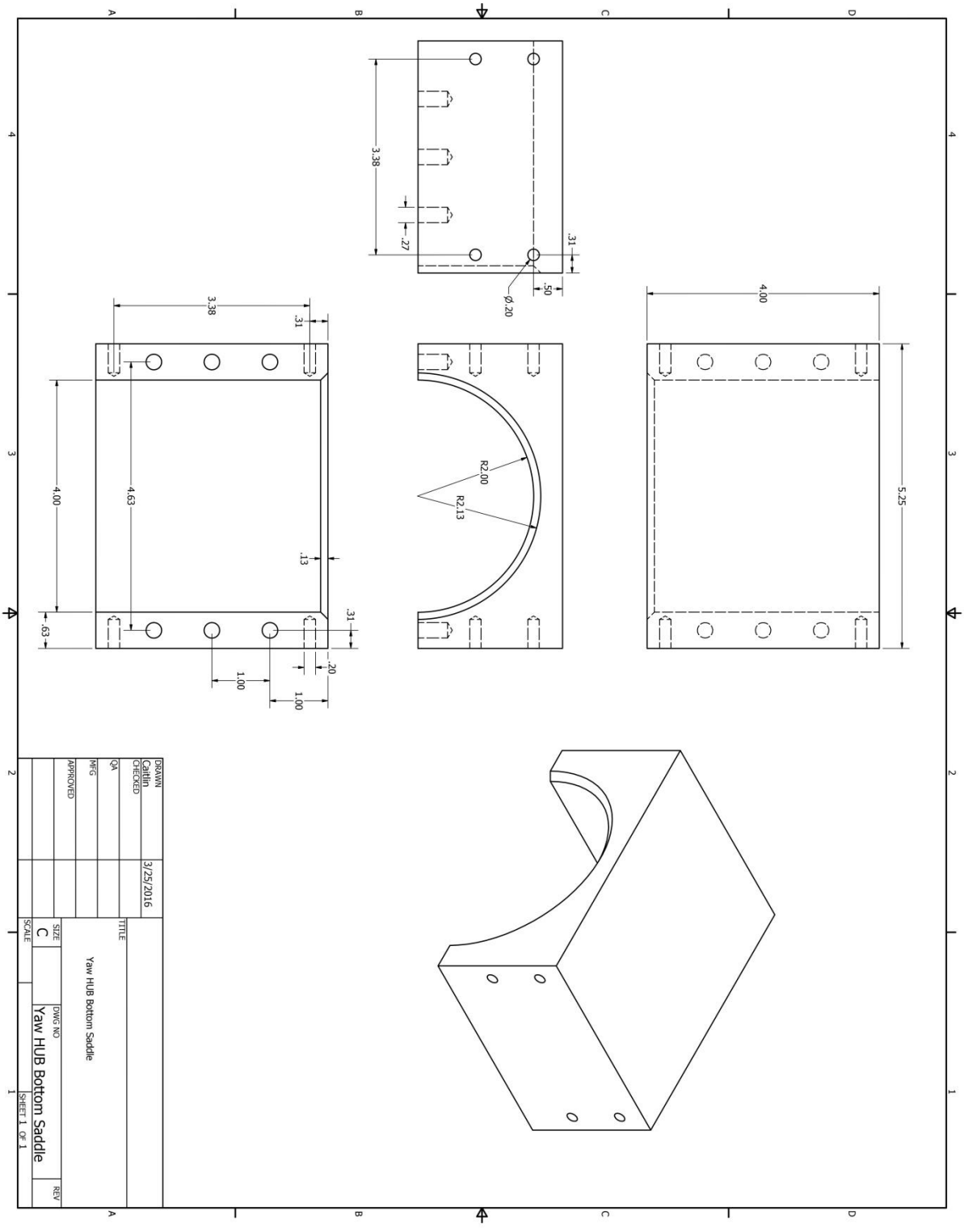

Figure 55: Yaw Hub Bottom Saddle

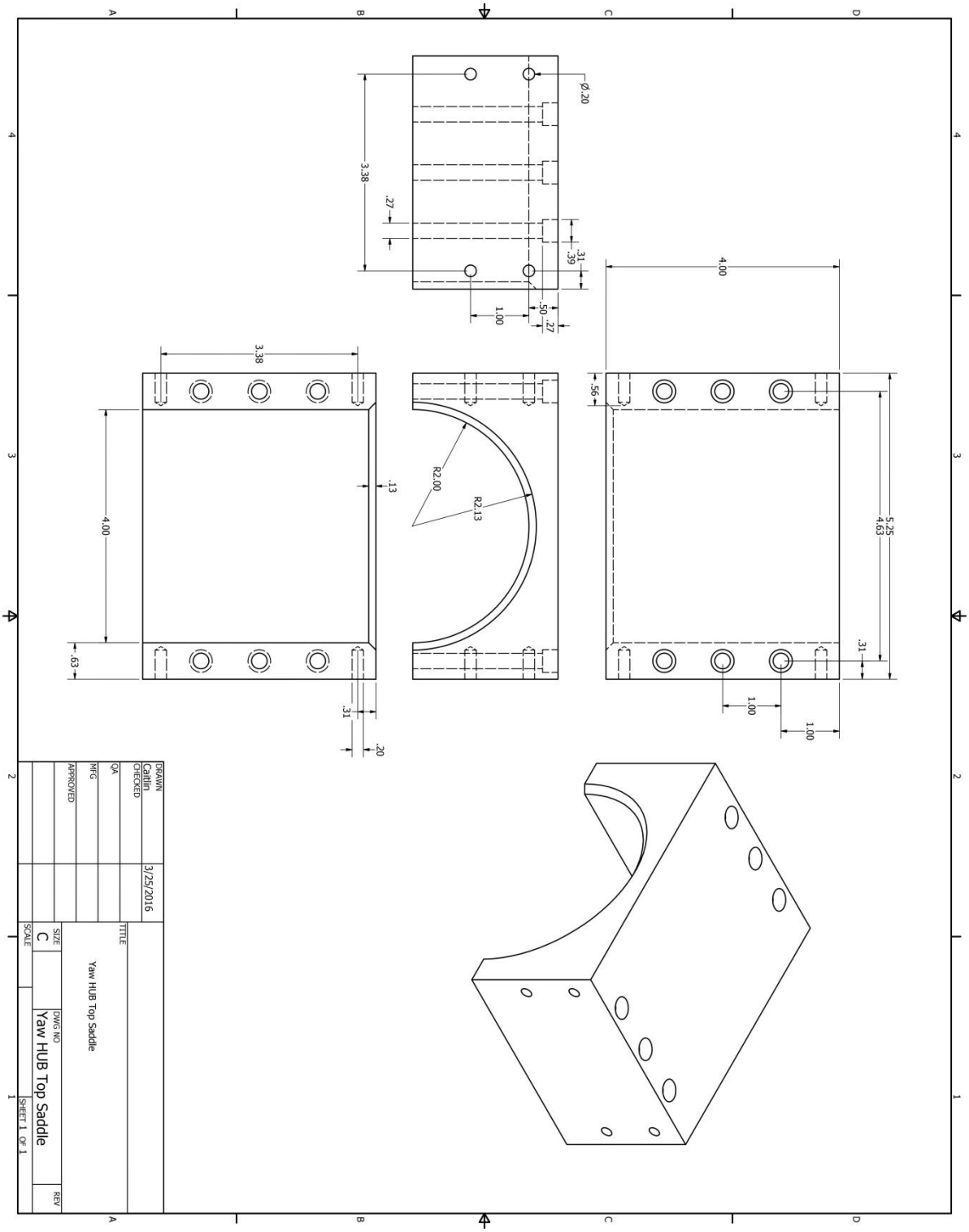

Figure 56: Yaw Hub Top Saddle

Appendix C

Appendix of Equations

$$A = (H * B) - (h * b) \tag{1}$$

$$I = \frac{1}{12}[(B * H^3) - (b * h^3)] \tag{2}$$

$$\%Wt = \left(\frac{A_i - A_0}{A_0}\right) * 100 \tag{3}$$

$$\%Stiff = \left(\frac{I_i - I_0}{I_0}\right) * 100 \tag{4}$$

$$Disp(x) = -\frac{Px(3L^2 - 4x^2)}{48EI} \tag{5}$$

$$Moment_{max} = -\frac{Pl}{4} \tag{6}$$

$$Stress_{max} = |Moment\_max| * \left(\frac{c}{I * 2}\right) \tag{7}$$

$$Shear_{max} = \frac{P}{2} \tag{8}$$

$$Margin = \left(\frac{theoretical_{max}}{calculated_{max}}\right) - 1 \tag{9}$$

$$\sigma_{xx} = \frac{E}{(1-2\nu)(1+\upsilon)}\left[(1-\upsilon)\varepsilon_{xx} + \nu\varepsilon_{yy} + \nu\varepsilon_{zz}\right] \tag{10}$$

$$\sigma_{yy} = \frac{E}{(1-2\nu)(1+\upsilon)}\left[\nu\varepsilon_{xx} + (1-\nu)\varepsilon_{yy} + \nu\varepsilon_{zz}\right] \tag{11}$$

$$\sigma_{zz} = \frac{E}{(1-2\nu)(1+\upsilon)}\left[\nu\varepsilon_{xx} + \nu\varepsilon_{yy} + (1-\nu)\varepsilon_{zz}\right] \tag{12}$$

$$\epsilon_x = \frac{\sigma_x}{E} - \nu\frac{\sigma_y}{E} - \nu\frac{\sigma_z}{E} \tag{13}$$

$$\epsilon_y = -\nu\frac{\sigma_x}{E} + \frac{\sigma_y}{E} - \nu\frac{\sigma_z}{E} \quad (14)$$

$$\epsilon_z = -\nu\frac{\sigma_x}{E} - \nu\frac{\sigma_y}{E} + \frac{\sigma_z}{E} \quad (15)$$

BIBLIOGRAPHY

[8] "Aluminium alloys - Alloys for extrusion", *Aluminiumdesign.net*. [Online]. Available: http://www.aluminiumdesign.net/design-support/aluminium-alloys-alloys-for-extrusion/. [Accessed: 10- Jun- 2015].

[9] "ASM Material Data Sheet", *Asm.matweb.com*, 2015. [Online]. Available: http://asm.matweb.com/search/SpecificMaterial.asp?bassnum=MA6061t6. [Accessed: 09- Jun- 2015].

[1] K. DeWeese and P. Ward, *DEMONSTRATION OF A BALLOON BORNE ARC-SECOND POINTER DESIGN*, 1st ed. College Park, MD: NASA Science Technology Conference (NSTC), 2007, p. https://esto.nasa.gov/conferences/nstc2007/.

[2] R. Garner, "WASP Gives NASA's Planetary Scientists New Observation Platform", *NASA*, 2014. [Online]. Available: http://www.nasa.gov/content/goddard/wasp-gives-nasas-planetary-scientists-new-observation-platform. [Accessed: 05- Jun- 2015].

[5] *HexWeb HONEYCOMB SANDWICH DESIGN TECHNOLOGY*, 1st ed. Dublin, CA: Hexcel Composites, 2000, pp. 11-13, 25-26.

[4] H. Kim, *The basics on bonded sandwich construction TSB 124*, 1st ed. Dublin, CA: Hexcel, 1987.

[3] "Modulus of Elasticity or Young's Modulus - and Tensile Modulus for some common Materials", *Engineeringtoolbox.com*. [Online]. Available: http://www.engineeringtoolbox.com/young-modulus-d_417.html. [Accessed: 09- Jun- 2015].

[7] "NASA Balloon Program Office Code 820", *Sites.wff.nasa.gov*, 2015. [Online]. Available: http://sites.wff.nasa.gov/code820/faq.html. [Accessed: 09- Jun- 2015].

[6] J. Thompson, "Effects Of Low Temperature on Performance of Steel & Equipment", *Sparta Engineering*, 2013. [Online]. Available: http://www.spartaengineering.com/effects-of-low-temperature-on-performance-of-steel-equipment/. [Accessed: 09- Jun- 2015].

ACADEMIC VITA

Caitlin E. Gibbons

PERSONAL STATEMENT

I am an adaptable and innovative qualified Mechanical Engineer with 5 years of experiences working in various different labs within the National Aeronautics and Space Administration (NASA). I am seeking to develop my expertise in mechanical design, simulation, and testing within Code 548 at NASA Wallops Flight Facility.

EDUCATION

- The Pennsylvania State University
  B.S. Mechanical Engineering
  Schreyer Honors College
  Thesis Title: Redesign to Reduce Mass: Wallops Arc-second Pointer (WASP)
  Thesis Supervisor: Dr. Sean Brennan

INTERNATIONAL EDUCATION

- The Pennsylvania State University
  Schreyer Honors College
  London Study Tour, THEA 490H 2016

- The National University of Singapore
  Mechanical Engineering Product Design Program 2014

EMPLOYMENT

Pathways Co-op: Engineering Student Trainee
NASA Wallops Flight Facility | Code 548 | Chincoteague, VA | https://aetd.gsfc.nasa.gov/code540/
June 2015 – Aug. 2014

Achievements
- Redesigned the Wallops Arc Second Pointer (WASP) to reduce mass using Autodesk Inventor Pro
- Documented research, design, developments, and assembly of WASP
- Researched shock/vibration sensors to update equipment
- Aided with educational outreach program, called WRATS, to show teachers how to build model rockets

Pathways Co-op: Engineering Student Trainee
NASA Goddard Space Flight Center | Code 548 | Greenbelt, MD | http://asd.gsfc.nasa.gov/bettii/
June 2014 – Aug. 2014

Achievements
- Redesigned a structure to hold the internal far-infrared optics for the Balloon Experimental Twin Telescope for Infrared Interferometry (BETTII) using Solid Works
- Invented a passive cooling system for a leach controller box
- Built a 10x10 foot clean room for future assembly of the dewar and internal optics

Mechanical Engineering Intern
NASA Goddard Space Flight Center | Code 665 | Greenbelt, MD | http://asd.gsfc.nasa.gov/bettii/
Aug. 2013 – Dec. 2013

Achievements
- Designed a structure to hold the internal far-infrared optics for BETTII using Solid Works
- Created a solid body model of the detector box for the internal near-infrared optics

Mechanical Engineering Intern
NASA Goddard Space Flight Center | Code 596 | Greenbelt, MD | https://aetd.gsfc.nasa.gov/code590/
June 2012 – Aug. 2012

Achievements
- Conducted and documented failure/stress analysis on electrical satellite components
- Documented best known lab and software procedures for future engineer use
- Modeled mechanical test bench components using Solid Edge
- Performed thermal vacuum tests on satellite components

Heliophysics Science Intern
NASA Goddard Space Flight Center | Code 673 | Greenbelt, MD | http://science.gsfc.nasa.gov/
June 2011 – Aug. 2011

Achievements
- Studied and validated a new solar cycle prediction method in the Heliophysics department
- Researched and wrote a paper evaluating the value of a manned mission to Mars

---

KEY SKILLS

Technical Skills
- SolidWorks
- Autodesk Inventor Pro
- Solid Edge
- Abaqus
- MATLAB
- OpenModelica
- EES
- KaleidaGraph
- iMovie
- Microsoft Suite

Certificates
- Penn State Learning Factory Safety/Power Tools Certification
- Penn State Learning Factory Machining Certification

Honors and Awards
- The Pennsylvania Space Grant Consortium Undergraduate Space Grant Scholarship 2015 – 2016
- Pentz Memorial Academic Excellence Scholarship 2012 – 2016
- Academic Excellence Scholarship 2012 – 2016
- NASA Pathways Co-op Scholarship 2014 – 2016
- Coleman George J Scholarship 2015
- National Space Club Scholars Award 2013
- South Carroll High School Outstanding Achievement in Science 2012

Language Proficiency

- English – Native
- Spanish – Intermediate

Community Service Involvement

- Mentor for Schreyer Career Development Program (CDP) 2014 – 2016
- Volunteer Librarian for Chincoteague Island Library, Virginia 2015
- Team Lead and Mentor for Schreyer Honors Orientation (SHO Time) 2013 – 2015
- Mentor for NASA INSPIRE Online Learning Community 2012 – 2013
- Springfield THON 2012 – 2013

PERSONAL INTERESTS

Traveling | Reading | Ceramics | Swing Dancing

REFERENCES

References are available on request.